International Electronic Journal of Pure and Applied Mathematics

Volume 1 No. 3 2010, 303-337

BIFURCATION AND CHAOS IN HIGHER DIMENSIONAL PIONEER-CLIMAX SYSTEMS

Yogesh Joshi[1 §], Denis Blackmore[2]

[1,2]Department of Mathematical Sciences
New Jersey Institute of Technology
Newark, NJ 07102-1982, USA
[1]e-mail: yj23@njit.edu
[2]e-mail: deblac@m.njit.edu

Abstract: A discrete dynamical model is formulated for the evolution of a biological system comprised of pioneer and climax species. This hierarchical model generalizes a well-known two-dimensional system for pioneer-climax species that provides reliable predictions for actual ecological systems. An extensive dynamical systems investigation is conducted using analytical and simulation tools. It is proved, for example, that the model has no Hopf bifurcations, but exhibits a rich array of flip (period-doubling) bifurcations for various (parameter) codimensions. A key to proving this and other results is that the hierarchical nature of the model makes it essentially equivalent to a sequence of one-dimensional systems when it comes to several dynamical properties (hierarchical principle). For example, this principle is used to prove chaos in the limit of a period-doubling cascade, shift map chaos on an invariant two-component Cantor set when there is a climax component, and the existence of an interesting small scale strange attractor like set when there is a pioneer component. Bifurcation diagrams and Lyapunov exponents are computed to further illustrate the chaotic dynamics, and it is indicated how chaos can be proved using higher dimensional horseshoe maps.

AMS Subject Classification: 37C05, 37G10, 37N25, 92D25
Key Words: pioneer and climax species, hierarchical principle, flip bifurcation, bifurcation diagrams, chaos, Lyapunov exponents

Received: June 8, 2010

§Correspondence author

International Electronic Journal of Pure and Applied Mathematics – IEJPAM, Volume 1, No. 3 (2010)

1. Introduction

Pioneer and climax species, which usually refer to types of flora, have been studied for many years by both ecologists and applied mathematicians, and more recently have been extensively investigated using a variety of dynamical systems models, most of which have been limited to two-dimensional (two-species) models. Those species that first colonize a barren land are called *pioneer species*. They are very hardy species that have adapted themselves to harsh conditions of nature, such as soil with less water retaining properties, and an overall dearth of water. To survive such harsh environments, in the course of time they tend to develop longer roots, leaves that transpire less, and other such adaptations. They are also the ones that usually grow first in an ecosystem which is destroyed by a forest fire, flood, earthquake, volcanic eruption or human intervention such as clearance of land for development and mining. They grow rapidly, but excessive increases in their density are detrimental to their own growth, leading ultimately to extinction. As the ecosystem grows with time, new species called *climax species* take over from the pioneer species. They now share the environment which was first occupied by the pioneer species. But they take more time to grow. The initial low density of climax species enhances their growth. Once they attain their maximum density, their growth rate starts to decline. Some examples of pioneer species are weeds, marram grass, some types of Pine and Poplar trees, wind-dispersed microbes, mosses and lichens that grow close to the ground. Hardwood trees like Oak, Maple, and White Spruce are examples of climax species [17], [18], [24].

Many experimental studies (field work) have also been conducted, with [8], [13], [14], [22] being some of the more recent ones. In [8], Jegan, Ramesh and Muthuchelian showed that pioneer species need light for regeneration and resprouting which are important processes that allow plant species to remain viable in an ecosystem, but which climax species do not require to the same extent. They evolve in an environment that is made easy to grow and thrive in by their predecessors, which are typically pioneer species. Jegan et al [8] classified their results based on forest openings (closed, small gap and large gap) which played a pivotal role in the study.

Raaimakers et al [13] investigated whether low phosphorous (P) availability limits the process of photosynthesis more than nitrogen (N) does in tree species in Guyana where the soil quality is acidic. The experiment was carried on nine pioneer and climax tree species. They also studied the relationship between leaf P and N content with photosynthetic capacity. They found at similar P and N content, pioneer species have a higher photosynthetic capacity than the climax species in a range of light climates. Photosynthetic characteristics and pattern of biomass accumulation in seedlings of pioneer and climax tree species from Brazil were studied by Silvestrini et al [22]. The seedlings were grown for four months under low light (5% to 8% sunlight) and high light (100% sunlight). Both species exhibited characteristics that favor growth under conditions that resemble their natural microenvironments.

International Electronic Journal of Pure and Applied Mathematics – IEJPAM, Volume 1, No. 3 (2010)

They also found that the climax species grow under high light, which is not normally observed in climax species. They proposed to explain this behavior using the spatio-temporal light regime of the forest. In [11], Kuijk developed and used a model for forest regeneration and restoration in Vietnam. The model evaluates shoot height and plant architecture, biomass allocation patterns and leaf physiology in terms of light capture and photosynthetic gains. Kuijk's model proved to be quite successful when applied to grasslands. Forest regeneration is a successional process where old trees (pioneers) are replaced by the new ones (climax) and a structural change in the forest canopy occurs.

From the applied mathematical perspective, the challenge is to formulate dynamical models for the evolution of ecosystems comprised of pioneer and climax species that can be used to reliably predict the behavior described above as well as a range of other qualitative and quantitative properties. Such models are usually either continuous or discrete dynamical systems, and the predictions are made using a variety of theoretical and computational tools that have been developed to analyze these models. Our approach here is to study a discrete dynamical systems model that is a higher dimensional generalization of a two-species system introduced by Selgrade and Namkoong [17, 18], which has proven to be quite successful in predicting the behavior of a pair of such species.

2. The Model

In an ecosystem, there are many interactions taking place such as animal-animal, plant-plant, and plant-animal that lead either to decline and possible extinction of one or more species (survival of the fittest) or coexistence (symbiosis). There also is another scenario, where some particular species of plants survive the harsh conditions (pioneer) of the environment and later on become extinct after making the environment more friendly for other species (climax), thus increasing their chances for survival. In the jargon of ecology this is called *succession*. Then after attaining maximum density, the climax species typically also start to dwindle. For more details, see [17], [18], [24].

This paper is inspired by the work of such researchers as Selgrade & Namkoong [17], [18], Franke & Yakubu [4], Sumner [23], [24], and Hassell & Comins [6] who have conducted extensive investigations of two-dimensional pioneer-climax systems. These authors usually combine all the individual population densities x_i of the species into a single entity, called the *total weighted density*, $z_i = \sum_{j=1}^{m} c_{ij}x_i$, where the $|c_{ij}|$ represent the intensity of the effect of the j-th population on the i-th. This helps to take into account all the competition (both interspecies and intraspecies) which takes place among the species. The c_{ij} are often called the *interaction coefficients*, and the c_{ii} are invariably chosen as positive numbers. So, while modeling an individual species, we will consider per capita growth rates to be

International Electronic Journal of Pure and Applied Mathematics – IEJPAM, Volume 1, No. 3 (2010)

functions of total weighted density. The per capita growth rate is called the *fitness function*, which can have the form

$$\phi(x) = x^{\alpha} e^{a-x},$$

and is shown in Figure 1, where $\alpha = 0$ or 1 according as the species is pioneer or climax, respectively, and a is a positive parameter describing the growth rate e^a of the species. For the i-th species to be a pioneer, it is required that the fitness function ϕ_i be smooth, monotonically decreasing and satisfies $\phi_i(0) > 1$. On the other hand, the species is climax if ϕ_i is smooth, initially monotonically increasing, reaches some maximum per capita growth rate, and deceases monotonically thereafter. Note that the density of species i is given as $x_i\phi_i(x_i)$. Typical growth of pioneer and climax species is shown in Figure 1. A widely accepted and studied 2-species pioneer-climax discrete dynamical model was introduced in Selgrade and Namkoong [17], [18]. Extending it to higher dimensions, we take the following m-dimensional pioneer-climax model ($m > 2$) as our starting point:

$$x_i(n+1) = x_i(n) z_i(n)^{\alpha_i} e^{a - z_i(n)}, \ (1 \le i \le m)$$

where

$$z_i = \sum_{j=1}^{m} c_{ij} x_j,$$

is the total weighted density, with $a_i,\ c_{ij} > 0$ and all $z_i^{\alpha_i} \ge 0$ whenever all $x_1, \ldots, x_m$ are nonnegative.

To make our results more relevant to real world ecosystems, we shall concentrate our attention by imposing *hierarchical competition* [2] on our model. In hierarchical competition, species i affects the growth of another species j if the j-th species lies below the i-th in the food chain of the ecosystem under consideration. To be more precise, our *hierarchical pioneer-climax model* (*HPCM*) assumes the form

$$x_i(n+1) = x_i(n) \left(\sum\nolimits_{j=1}^{i} c_{ij} x_j(n) \right)^{\alpha_i} \exp\left(a_i - \sum\nolimits_{j=1}^{i} c_{ij} x_j(n) \right) \tag{1}$$

($1 \le i \le m$). The system may be recast into discrete dynamical form in terms of the iterates of a smooth ($= C^{\infty}$) map – which is actually real-analytic ($= C^{\omega}$) – by defining $F_{\boldsymbol{\alpha},\boldsymbol{\nu}} : \mathbf{R}_+^m \to \mathbf{R}_+^m$ as

$$\begin{aligned} F_{\boldsymbol{\alpha},\boldsymbol{\nu}}(\boldsymbol{x}) = (f_{1\boldsymbol{\alpha},\boldsymbol{\nu}}(x_1), f_{2\boldsymbol{\alpha},\boldsymbol{\nu}}(x_1,x_2), \ldots, f_{m\boldsymbol{\alpha},\boldsymbol{\nu}}(\boldsymbol{x})) := (x_1 (c_{11}x_1)^{\alpha_1} \\ \times \exp(a_1 - c_{11}x_1), \ldots, x_m \left(\textstyle\sum_{j=1}^{m} c_{ij}x_j\right)^{\alpha_m} \exp\left(a_m - \textstyle\sum_{j=1}^{m} c_{ij}x_j\right)), \end{aligned} \tag{2}$$

where $\boldsymbol{x} := (x_1, \ldots, x_m) \in \mathbf{R}_+^m := \{\boldsymbol{x} \in \mathbf{R}^m : x_1, \ldots, x_m \ge 0\}$, $\boldsymbol{\alpha} := (\alpha_1, \ldots, \alpha_m)$, and the parameters are all grouped into $\boldsymbol{\mu} := (a_1, \ldots, a_m, c_{11}, c_{12}, \ldots, c_{1m}, \ldots, c_{m1},$

International Electronic Journal of Pure and Applied Mathematics – IEJPAM, Volume 1, No. 3 (2010)

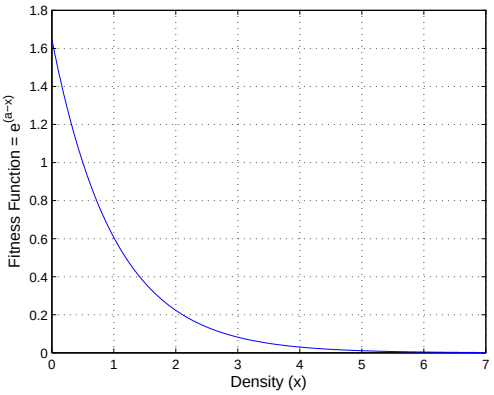

(a) Pioneer growth, with parameter $a = 0.5$

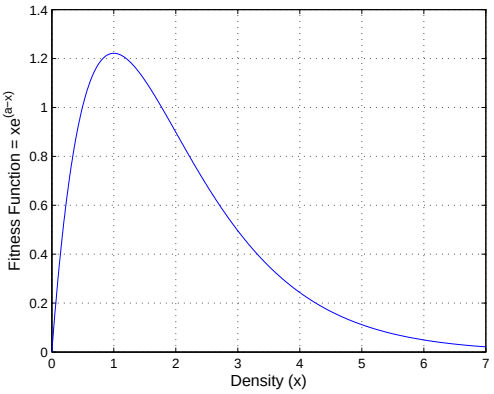

(b) Climax growth, with parameter $a = 1.2$

Figure 1: Growth of pioneer and climax species

$c_{m2}, \ldots, c_{mm}$). With this, we may rewrite (1) in difference/discrete dynamical system form as

$$\boldsymbol{x}_{n+1} = F_{\boldsymbol{\alpha},\boldsymbol{\nu}}(\boldsymbol{x}_n) \Longleftrightarrow \boldsymbol{x}_n = F^n_{\boldsymbol{\alpha},\boldsymbol{\nu}}(\boldsymbol{x}_0), \tag{3}$$

where $F^n_{\boldsymbol{\alpha},\boldsymbol{\nu}}$ denotes the usual n-fold composition of $F_{\boldsymbol{\alpha},\boldsymbol{\nu}}$ with itself, which is defined for all nonnegative integers and for negative integers when the inverse $F^n_{\boldsymbol{\alpha},\boldsymbol{\nu}}$ exists. We note here for future reference that the subscripts $\boldsymbol{\alpha}$ and $\boldsymbol{\mu}$ can and will be omitted when they are given and fixed for a particular investigation.

International Electronic Journal of Pure and Applied Mathematics – IEJPAM, Volume 1, No. 3 (2010)

3. Basic Dynamical Properties

In this section we explore some basic dynamical properties of our HPCM including simplifications, invariant sets, stability of fixed points and the like. We shall also describe how the hierarchical nature of the system reduces many dynamical considerations to one-dimensional maps obtained from the coordinate functions of (2). By way of simplification, it is easy to see that our map (2) is conjugate via the simple scaling $h(x_1, \ldots, x_m) := (x_1/c_{11}, \ldots, x_m/c_{mm})$ to a map of precisely the same form with

$$c_{11} = c_{22} = \cdots = c_{mm} = 1, \tag{U}$$

so we shall assume this to be the case from this point onward.

3.1. Invariant Sets

It is clear that the map (2) is actually defined on all of Euclidean m-space $\mathbf{R}^m$, and it follows directly from our assumptions that $F_{\boldsymbol{\alpha},\boldsymbol{\nu}}(\mathbf{R}^m_+) = \mathbf{R}^m_+$, so $\mathbf{R}^m_+$ is $F_{\boldsymbol{\alpha},\boldsymbol{\nu}}$-invariant, as well it should be since there should be no populations of negative size. Moreover, it is obvious from (2) that the origin, and all of the coordinate lines, planes and hyperplanes $x_{i_1} = x_{i_2} = \cdots = x_{i_k} = 0$, where $i_1, i_2, \ldots, i_k$, with $1 \leq k < m$, is any selection of k distinct elements of the set $\{1, 2, \ldots, m\}$ are F-invariant. There appear to be no other subsets that are obviously invariant by inspection without additional specializing restrictions on F.

3.2. Fixed Points

As noted above, the origin is obviously a fixed point of F for any choice of α and the parameter $\boldsymbol{\mu}$. Any additional fixed points are, by definition, solutions of

$$\boldsymbol{x} = F(\boldsymbol{x}) \Longleftrightarrow x_i = x_i \left(\sum\nolimits_{j=1}^{i} c_{ij}x_j\right)^{\alpha_i} \exp\left(a_i - \sum\nolimits_{j=1}^{i} c_{ij}x_j\right) \tag{4}$$

$(1 \leq i \leq m)$. Thus if $x_i \neq 0$, it must follow that

$$\left(\sum\nolimits_{j=1}^{i} c_{ij}x_j\right)^{\alpha_i} \exp\left(a_i - \sum\nolimits_{j=1}^{i} c_{ij}x_j\right) = 1,$$

which in the case of a pioneer component ($\alpha_i = 0$) is easily seen to be equivalent to

$$\sum\nolimits_{j=1}^{i} c_{ij}x_j = a_i; \tag{5}$$

on the other hand, when the component is climax ($\alpha_i = 1$), one finds that

$$\sum\nolimits_{j=1}^{i} c_{ij}x_j = V^{-1}\left(e^{-a_i}\right) = -W\left(-e^{-a_i}\right), \tag{6}$$

International Electronic Journal of Pure and Applied Mathematics – IEJPAM, Volume 1, No. 3 (2010)

as long as $a_i \geq 1$ so that the "inverse" V^{-1} of the function $V(s) = se^{-s}$ is defined for $s \geq 0$. Observe that $V^{-1}(u) = -W(-u)$, where W is the Lambert function [25], and $V^{-1}(0) = 0$, $V^{-1}(e^{-1}) = 1$ and $V^{-1}(u) = \{s_l(u), s_r(u)\}$ when $0 < u < e^{-1}$, with $0 < s_l < 1 < s_r$, and $s_l \downarrow 0$ and $s_r \uparrow \infty$ as $u \downarrow 0$.

In virtue of (4)-(6), finding the fixed points of F is a simple matter of solving a system of linear equations. We now consider a couple examples to illustrate this. Suppose first that all of the coordinate functions are pioneer (the all-pioneer case). Then it is easy to show, keeping in mind the assumption (U), that the unique fixed point with all nonzero coordinates is $(\hat{x}_1, \ldots, \hat{x}_m) = (a_1, (a_2 - c_{21}a_1), \ldots, (a_m - c_{m1}\hat{x}_1 - \cdots - c_{m,m-1}\hat{x}_{m-1}))$. As another example, we consider a 3-dimensional system in which the first two species are pioneer and the third is climax with $a_3 > 1$. In this case there are a pair of fixed points with all nonzero coordinates; namely $(\hat{x}_1, \hat{x}_2, \hat{x}_3) = (a_1, (a_2 - c_{21}\hat{x}_1), (s_l(e^{-a_3}) - c_{31}\hat{x}_1 - c_{32}\hat{x}_2))$ and $(\hat{x}_1, \hat{x}_2, \hat{x}_3) = (a_1, (a_2 - c_{21}\hat{x}_1), (s_r(e^{-a_3}) - c_{31}\hat{x}_1 - c_{32}\hat{x}_2))$. In a similar fashion, all fixed points of the HPCM involving any combination of pioneer and climax species can be computed.

The linear stability of any fixed point of the system is determined from a spectral analysis of the derivative (Jacobian) $m \times m$ matrix

$$F'_{\boldsymbol{\alpha},\boldsymbol{\nu}}(\boldsymbol{x}) = \left(\partial_{x_j} f_{i\boldsymbol{\alpha},\boldsymbol{\nu}}(x_1, \ldots, x_i)\right). \tag{7}$$

This is a lower triangular matrix since $\partial_{x_j} f_{i\boldsymbol{\alpha},\boldsymbol{\nu}}(x_1, \ldots, x_i) = 0$ when $i < j$; the diagonal entries (which are the eigenvalues) are

$$\partial_{x_i} f_{i\boldsymbol{\alpha},\boldsymbol{\nu}}(x_1, \ \ldots, \ x_i) = \begin{cases} (1 - c_{ii}x_i) \exp\left(a_i - \sum_{j=1}^{i} c_{ij}x_j\right), & \alpha_i = 0; \\ \left(\sum_{j=1}^{i} c_{ij}x_j\right) \left[c_{ii}x_i + (1 - c_{ii}x_i)(\sum_{j=1}^{i} c_{ij}x_j)\right] & \\ \times \exp\left(a_i - \sum_{j=1}^{i} c_{ij}x_j\right), & \alpha_i = 1. \end{cases}$$

and the entries below the diagonal ($i > j$) are

$$\partial_{x_j} f_{i\boldsymbol{\alpha},\boldsymbol{\nu}}(x_1, \ldots, x_i) = \begin{cases} -c_{ij}x_i \exp\left(a_i - \sum_{j=1}^{i} c_{ij}x_j\right), & \alpha_i = 0; \\ c_{ij}x_i \left(1 - \sum_{j=1}^{i} c_{ij}x_j\right) & \\ \times \exp\left(a_i - \sum_{j=1}^{i} c_{ij}x_j\right), & \alpha_i = 1. \end{cases}$$

Using formula (7) and the diagonal entries (see above), it is easy to characterize the linear stability of any fixed point of $F_{\boldsymbol{\alpha},\boldsymbol{\nu}}$, thereby obtaining a complete set of results of which the following two are just examples:

International Electronic Journal of Pure and Applied Mathematics – IEJPAM, Volume 1, No. 3 (2010)

Lemma 3.1. *For the m-dimensional all-pioneer model, the origin $\boldsymbol{x} = 0$ is a repeller (attractor) if $a_1, \ldots, a_m > 0$ ($a_1, \ldots, a_m < 0$), and for the all-climax case, the origin is superstable (all eigenvalues zero) for all values of $a_1, \ldots, a_m$.*

Lemma 3.2. *For the m-dimensional all-pioneer HPCM, the unique fixed point with positive coordinates $(\hat{x}_1, \ldots, \hat{x}_m)$ described above is stable if $|1 - \hat{x}_i| < 1$ for all $1 \leq i \leq m$, and unstable if any of $|1 - \hat{x}_i| > 1$.*

3.3. Possible Bifurcations

As is usual, we are interested in bifurcations of our dynamical system caused by variation of the parameters. We show in the next section that flip (period-doubling) bifurcations are quite ubiquitous for the HPCM. However, most other standard bifurcations cannot occur, and this includes the (codimension-1) Andronov-Hopf (or Neimark-Sacker) bifurcation, which occurs in numerous other dynamical systems models of physical and biological phenomena.

Lemma 3.3. *There are no Hopf bifurcations for the HPCM.*

Proof. It follows from (3.2) that all eigenvalues of $F'_{\boldsymbol{\alpha},\boldsymbol{\nu}}$ are real, which precludes the existence of Hopf bifurcations. □

We note here that it is actually not too difficult prove that a general (non-hierarchical) discrete dynamical system of pioneer-climax evolution of the type under consideration here cannot have a Hopf bifurcation if all of the interaction coefficients are nonnegative. However, since this does not really play any role in the sequel, we prefer not to go into this here. On the other hand, if some of the interaction coefficients are negative, the system can experience an Andronov-Hopf (or Neimark-Sacker) bifurcation as illustrated in the following (cf. [24]):

Example 3.4. Consider $F : \mathbf{R}^2_+ \to \mathbf{R}^2_+$ defined as

$$F(x, y; \mu) := \left(x \exp\left((8/3) + \mu - x - y\right), y \exp\left((4/3) + (\mu/2) + x - y\right)\right),$$

where μ is just a real number. It is straightforward to verify that this map has a supercritical Hopf bifurcation for the fixed point $(2/3, 2)$ at $\mu = 0$.

3.4. The Hierarchical Principle

Owing to the hierarchical nature of the map $F_{\boldsymbol{\alpha},\boldsymbol{\nu}}$, the analysis of several important dynamical aspects of the system (3) can be reduced to a sequence of calculations involving the (1-dimensional) coordinate functions of the map. This amounts to what is essentially a reduction of the analysis of an m-dimensional system to that of a 1-dimensional system as a result of the hierarchical structure. We shall in the sequel make extensive use of this property, which we call the *hierarchical principle*, or *h-principle*. Let us describe how this h-principle works for fixed points, periodic

International Electronic Journal of Pure and Applied Mathematics – IEJPAM, Volume 1, No. 3 (2010)

points, and the existence of chaotic regimes, and leave it to the reader to fathom the analogs for other types of dynamical phenomena such as bifurcations.

First, suppose we wish to find a fixed point of the system. We may start by obtaining a fixed point of the 1-dimensional first coordinate function $f_{1\boldsymbol{\alpha},\boldsymbol{\nu}}$, then substituting this, call it $\hat{x}_1$, in the second coordinate function $f_{2\boldsymbol{\alpha},\boldsymbol{\nu}}$ to get a 1-dimensional map depending only on x_2, for which we find a fixed point $\hat{x}_2$. Then we substitute $\hat{x}_1$ and $\hat{x}_2$ into $f_{3\boldsymbol{\alpha},\boldsymbol{\nu}}$ to obtain a function only of x_3. Repeating this process until we exhaust the list of coordinate functions, we obtain a fixed point $(\hat{x}_1, \hat{x}_2, \ldots, \hat{x}_m)$ of $F_{\boldsymbol{\alpha},\boldsymbol{\nu}}$, and all of its fixed points can be obtained in this manner. Now there is nothing special about starting with the first coordinate function: Assuming the $(\hat{x}_1, \ldots, \hat{x}_{k-1})$ is a fixed point of the $(k-1)$-dimensional map defined by the first $(k-1)$ coordinate functions of $F_{\boldsymbol{\alpha},\boldsymbol{\nu}}$, we can pick up the above process by substituting $\hat{x}_1, \ldots, \hat{x}_{k-1}$ in $f_{k\boldsymbol{\alpha},\boldsymbol{\nu}}$ to obtain a function only of x_k. Then we can find a fixed point of this map, substitute it in the next coordinate map, and so on to obtain a fixed point for (2).

To find a periodic point of $F_{\boldsymbol{\alpha},\boldsymbol{\nu}}$ of (least) period k, it suffices to observe that $F^k_{\boldsymbol{\alpha},\boldsymbol{\nu}}$ also is hierarchical. Accordingly the period k points can be computed as fixed points of $F^k_{\boldsymbol{\alpha},\boldsymbol{\nu}}$ in the same succession of 1-dimensional calculations as described for fixed points of $F_{\boldsymbol{\alpha},\boldsymbol{\nu}}$, and once again we essentially have a reduction from m-dimensions to 1-dimension as a result of the hierarchical structure. Finally, it is easy to see that chaos for the full system is generated by chaos in any of the coordinate maps, say $f_{k\boldsymbol{\alpha},\boldsymbol{\nu}}$. All we need do is set $(\hat{x}_1, \ldots, \hat{x}_{k-1}) = (0, \ldots, 0)$, which is a fixed point for the map defined by the first $(k-1)$ coordinate functions, and consider the 1-dimensional map $\hat{f}_k(x_k) := f_{k\boldsymbol{\alpha},\boldsymbol{\nu}}(0, \ldots, 0, x_k)$. Then a chaotic orbit for $\hat{f}_k$ naturally leads to a chaotic orbit for $F_{\boldsymbol{\alpha},\boldsymbol{\nu}}$, the simplest of which has $x_{k+1} = \cdots = x_m = 0$.

4. Period-Doubling Bifurcation

We shall now study the most significant bifurcations that can occur in the HPCM at considerable length. In order to simplify the analysis here and in succeeding sections, we shall confine our attention to 3-dimensional pioneer-climax systems, wherein we redesignate a_1, a_2 and a_3 as a, b and c, respectively. This entails no real loss of generality, for all of our results and conclusions can be extended to the m-dimensional case in an entirely straightforward fashion.

As mentioned above, most of the interesting bifurcation behavior of the HPCM is confined to period-doubling bifurcations. The phenomenon of a *period-doubling bifurcation* (or *flip bifurcation*) occurs in many discrete dynamical systems, and we expect it to occur in our model based upon numerous numerical simulations and experimental evidence. In period-doubling bifurcation, a fixed point becomes unstable (stable) and creates a stable (unstable) 2-cycle. Well-known criteria for such bifurcations are given in the following result (see [26]):

International Electronic Journal of Pure and Applied Mathematics – IEJPAM, Volume 1, No. 3 (2010)

Theorem 4.1. *The following are sufficient conditions for the occurrence of a period-doubling bifurcation in a 1-parameter family of $C^r(r \geq 3)$ 1-dimensional maps*

$$x(k+1) = f(x(k),\ \mu), \quad x \in \mathbb{R}, \quad \mu \in \mathbb{R},\ k \geq 0 :$$

$f(x^*,\ \mu^*) = x^*$, $f_x(x^*,\ \mu^*) = -1$, $f^2_\mu(x^*,\ \mu^*) = 0$, $f^2_{xx}(x^*,\ \mu^*) = 0$, $f^2_{x\mu}(x^*,\ \mu^*) \neq 0$, *and* $f^2_{xxx}(x^*,\ \mu^*) \neq 0$, *where x^* is the fixed point and μ^* is the bifurcation value.*

We now study flip bifurcations in detail: starting with the one-dimensional model and then generalizing the result to the 3-dimensional case in a step-by-step manner. In light of the h-principle, it makes sense to begin by considering 1-dimensional pioneer and climax maps represented in the form $f, g : \mathbf{R}_+ \to \mathbf{R}_+$, where

$$f(x) = f(x; a) := xe^{a-x} \tag{8}$$

and

$$g(x) = g(x; a) := x^2 e^{a-x} \tag{9}$$

respectively where a is a positive parameter that we vary, and we have taken (U) into account. For our analysis of flip bifurcations, we could use Theorem 4.1, but we shall find it more convenient to provide direct proofs – revealing more aspects of the dynamics – that take full advantage of the special forms of the maps (8) and (9).

First, we characterize the fixed points of the two functions. **Lemma 4.2.** *The map f given by (8) has precisely two fixed points: $x = 0$ and $x = a$, with $f'(0) = e^a$ and $f'(a) = 1 - a$, so the origin is always unstable, and a is stable (unstable) if $|1 - a|$ is less than (greater than) one. On the other hand, the function (9) always has 0 as a superstable fixed point, and this is the only fixed point if $a < 1$. If $a = 1$, g also has the fixed point $x = 1$, with $g'(1) = 1$ which is unstable from the left, but stable from the right. If $a > 1$, g has the superstable fixed point 0, and an unstable fixed point at the smaller of the two positive solutions x_l of*

$$xe^{a-x} = 1$$

for which $0 < x_l < 1$, and another fixed point x_r at the larger of the two solutions ($x_r > 1$), which is stable or unstable according as the absolute value of $g'(x_r) = x_r(2 - x_r)e^{a-x_r}$ is less than or greater than one, respectively.

Proof. The solutions of

$$f(x) = xe^{a-x} = x,$$

are obviously $x = 0$ and $x = a$, which are the fixed points of f. The stability results for these fixed points of f follows from the formula for the derivative

$$f'(x) = (1 - x)e^{a-x}.$$

International Electronic Journal of Pure and Applied Mathematics – IEJPAM, Volume 1, No. 3 (2010)

The fixed points of g are the nonnegative solutions of

$$g(x) = x^2 e^{a-x} = x,$$

so $x = 0$ is always a solution. For positive solutions, we can divide the above by x to obtain

$$h(x) := xe^{a-x} = 1.$$

A simple calculation shows that the maximum of h is e^{a-1}, which occurs at $x = 1$. The remaining results concerning the positive fixed points of g follow from this formula, the derivative

$$g'(x) = x(2-x)e^{a-x}$$

and a simple cobweb argument for the fixed point x_l, so the proof is complete. □

A necessary condition for a flip bifurcation to occur at a fixed point is that the derivative be equal to -1. Relevant to this is our next result, which follows directly from Lemma 4.1 and the above proof. We leave the elementary verification to the reader.

Lemma 4.3. *The fixed point a is stable for $0 < a < 2$. The derivative $f'(a) = -1$ at $a = 2$, and decreases thereafter, so a is unstable for $a > 2$. The derivative $g'(x_r)$ is a decreasing function of a, starting at $g'(x_r) = 1$ when $a = 1$ and $x_l = x_r = 1$, and $g'(x_r) \to -\infty$ as $a \to \infty$. Consequently, there is a unique value of $a > 1$ where $g'(x_r) = -1$; namely, $x_r = 3$, which corresponds to $a = 3 - \ln 3$.*

We next prove that a supercritical flip bifurcation occurs at the fixed points of f and g at which derivatives are equal to -1. Recall that by supercritical we mean that a fixed point transitions from stable to unstable across the bifurcation value of a, and gives birth to a stable 2-cycle.

Theorem 4.4. *Both the pioneer map $f(x) = xe^{a-x}$ and the climax map $g(x) = x^2 e^{a-x}$ have supercritical flip bifurcations at their largest fixed points given by $x_p = a$ and $x_c = 3$, respectively, when $f'(x_p) = -1$ and $g'(x_c) = -1$ for $a = 2$ and $a = 3 - \ln 3$.*

Proof. We give the proof only for the pioneer case since the argument for the climax function is completely analogous (although admittedly rather more complicated). Thus, we only deal with the bifurcation at the fixed point $x = a$ of $f(x) = xe^{a-x}$ as the parameter crosses $a = 2$. To show the flip bifurcation, we study f and f^2, where

$$f^2(x) := f(f(x)) = (xe^{a-x}) \exp(a - xe^{a-x})$$

for $a > 2$. Of course, as $x = a$ is a fixed point of f, it is also a fixed point of f^2. It follows from Lemma 4.3 that f has a unique fixed point in a neighborhood of $x = a$, and $x = a$ is an unstable fixed point of f for $a > 2$; therefore, it is also an unstable fixed point of f^2 since $f^{2\prime}(a) = (f'(a))^2 > 1$ for $a > 2$. We now show

International Electronic Journal of Pure and Applied Mathematics – IEJPAM, Volume 1, No. 3 (2010)

that f^2 has additional fixed points $x_*^{(-)} < \hat{x} = 2+\mu < x_*^{(+)}$ when μ is a sufficiently small positive number such that $x_*^{(-)},\ x_*^{(+)} \to 2$ as $\mu \to 0$. Clearly, this implies that $\{x_*^{(-)},\ x_*^{(+)}\} = \{x_*^{(-)},\ f(x_*^{(-)})\} = \{f(x_*^{(+)}),\ x_*^{(+)}\}$ is a 2-cycle of f. The fixed points of f^2 near $x = a$, satisfy

$$xe^{a-x}\exp(a - xe^{a-x}) = x,$$

and since $x \neq 0$, this is equivalent to

$$\exp[2a - x(1 + e^{a-x})] = 1,$$

which holds iff

$$2a - x(1 + e^{a-x}) = 0. \tag{10}$$

It is easy to see that $x = a$ is a solution of (10) for every $a > 0$. Let us now consider this equation with $a = 2 + \mu$ for small nonnegative values of μ, so that if $x = a + y = 2 + \mu + y$, we have

$$\psi(y) = \psi(y;\ \mu) := 2(2+\mu) - [(2+\mu) + y][1 + e^{-y}] = 0. \tag{11}$$

Clearly $y = 0$ is a solution of (11) for every $\mu \geq 0$, and this corresponds to the fixed point $x = \hat{x} = a$ of f. But, there are two other solutions that comprise a (nontrivial) 2-cycle of f. Noting that $\psi(0;\ \mu) = 0$ for all $\mu \geq 0$, $\psi \to -\infty$ as $y \to +\infty$, $\psi \to +\infty$ as $y \to -\infty$, $\frac{d\psi}{dy}(0;\ \mu) = \mu$, and performing a more detailed curve plotting analysis, we find that graph of ψ has the form shown below for $\mu > 0$. Accordingly it has a positive and negative zero $y^{(+)} = y^{(+)}(\mu)$ and $y^{(-)} = y^{(-)}(\mu)$, respectively, for every sufficiently small positive value of the parameter μ. To find the nature of these zeros, we assume series solutions of the form

$$y^{(-)} = \sum_{k=1}^{\infty} a_k^{(-)}\sigma^k,\ y^{(+)} = \sum_{k=1}^{\infty} a_k^{(+)}\sigma^k,$$

where $\sigma = \sqrt{\mu}$ $(\mu \geq 0)$. We then substitute these series in (11), wherein we use the expansion $e^{-y} = \sum_{k=0}^{\infty} \frac{(-1)^k y}{k!}$, to obtain

$$\begin{aligned}
\psi &= 2(2+\sigma^2) - [(2+\sigma^2) + y][2 + \sum_{k=1}^{\infty} \frac{(-1)^k y^k}{k!}] = 0,\\
&-\sigma^2 + \frac{\sigma^2 y}{2} + \frac{1}{3!}(1-\sigma^2)y^2 + \frac{1}{4!}(1-\sigma^2)y^3 + \cdots = 0,\\
&-\sigma^2 + \frac{\sigma^2}{2}\sigma\left(\sum_{k=1}^{\infty} a_k\sigma^{k-1}\right) + \frac{1}{3!}(1-\sigma^2)\sigma^2\left(\sum_{k=1}^{\infty} a_k\sigma^{k-1}\right)^2\\
&+ \frac{1}{4!}(1-\sigma^2)\sigma^2\sigma\left(\sum_{k=1}^{\infty} a_k\sigma^{k-1}\right)^3 + \cdots = 0,
\end{aligned}$$

International Electronic Journal of Pure and Applied Mathematics – IEJPAM, Volume 1, No. 3 (2010)

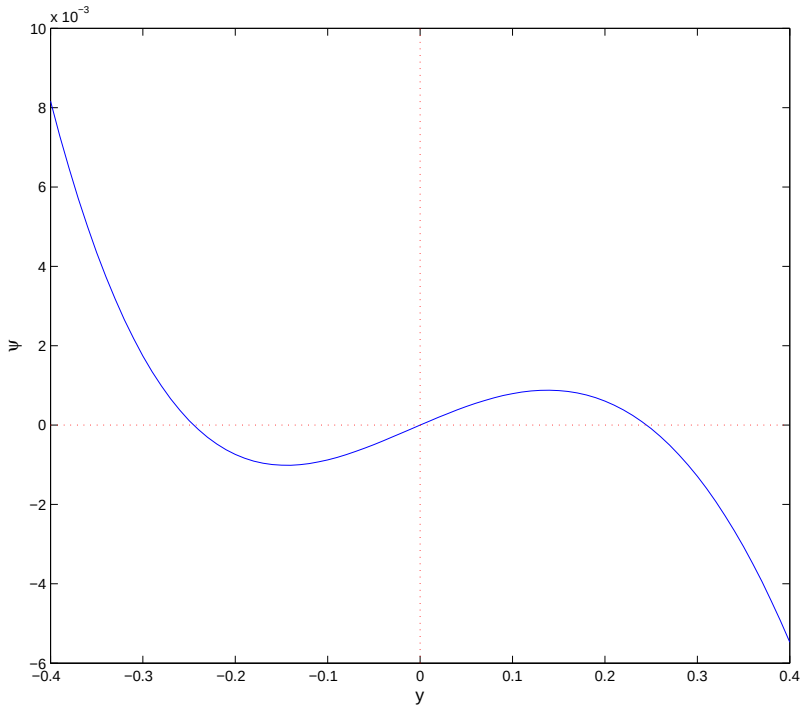

Figure 2: ψ as a function of y for $\mu = 0.01$

$$-1+\frac{1}{2}\sigma\left(\sum_{k=1}^{\infty}a_k\sigma^{k-1}\right)+\frac{1}{3!}(1-\sigma^2)\left(\sum_{k=1}^{\infty}a_k\sigma^{k-1}\right)^2$$
$$+\frac{1}{4!}(1-\sigma^2)\sigma\left(\sum_{k=1}^{\infty}a_k\sigma^{k-1}\right)^3+\cdots=0,$$

which can be solved recursively to yield $a_1 = \pm\sqrt{6},\ a_2 = 0,\ \cdots$, etc. So, we see that $y^{(-)},\ y^{(+)}$ are analytic in $\sqrt{\mu}$ for $\mu \geq 0$ sufficiently small, and

$$y^{(-)} = -\sqrt{\mu}\left[\sqrt{6}+O(\mu)\right],$$
$$y^{(+)} = \sqrt{\mu}\left[\sqrt{6}+O(\mu)\right] \text{ as } \mu \downarrow 0.$$

Therefore, in addition to the fixed point $\hat{x} = 2+\mu$ of f, f^2 has another pair of fixed points $x_*^{(-)} = 2-\sqrt{6\mu}+O(\mu) < \hat{x} < x_*^{(+)} = 2+\sqrt{6\mu}+O(\mu)$ for sufficiently small $\mu \geq 0$. Hence, $\{x_*^{(-)},\ x_*^{(+)}\}$ is a (nontrivial) 2-cycle for f for suf-

International Electronic Journal of Pure and Applied Mathematics – IEJPAM, Volume 1, No. 3 (2010)

ficiently small positive μ, and this is stable since it is easy to verify that $|f^{2\prime}(x_*^{(-)})| = |f'(x_*^{(-)})f'(x_*^{(+)})| < 1$ for $\mu > 0$ sufficiently small. Thus the proof is complete. □

4.1. Codimension – One Flip Bifurcations

We now use the above results to show that if any of the parameters $a,\ b$ or c varies, while the other two are fixed, the whole system exhibits a supercritical flip bifurcation. The dynamics of our discrete hierarchical system is determined by the iterates of the map $F : \mathbf{R}^3_+ \to \mathbf{R}^3_+$ defined as

$$F(x) = F(x_1,\ x_2,\ x_3) = (f_1(x_1;\ a),\ f_2(x_1,\ x_2;\ b),\ f_3(x_1,\ x_2,\ x_3;\ c)), \tag{12}$$

where $f_1,\ f_2,\ f_3$ are either pioneer or climax type functions, and we have indicated only the dependence on the positive parameters $a,\ b$ and since we are assuming that only they, and not the interaction coefficients c_{ij} are allowed to vary.

Recall that the derivative matrix of F at any point can be represented by the triangular Jacobian matrix

$$F'(x) = \begin{pmatrix} \frac{\partial f_1}{\partial x_1} & 0 & 0 \\ \frac{\partial f_2}{\partial x_1} & \frac{\partial f_2}{\partial x_2} & 0 \\ \frac{\partial f_3}{\partial x_1} & \frac{\partial f_3}{\partial x_2} & \frac{\partial f_3}{\partial x_3} \end{pmatrix} \tag{13}$$

with eigenvalues $\lambda_1 = \frac{\partial f_1}{\partial x_1}(x),\ \lambda_2 = \frac{\partial f_2}{\partial x_2}(x),\ \lambda_3 = \frac{\partial f_3}{\partial x_3}(x)$ that may be viewed as associated with the parameters $a,\ b$ and c respectively. Our codimension-one generalization of Theorem 4.4 is the following result, which is proved in Appendix.

Theorem 4.5. *Let one of the three eigenvalues be equal to -1 and the other two eigenvalues be less than one in absolute value at a fixed point of F. Let $v = a,\ b$ or c be the parameter associated with eigenvalue equal to -1. Then there is a bifurcation value v_* and corresponding fixed point $\hat{x}$ of F giving rise to a supercritical flip bifurcation.*

4.2. Codimension – Two Flip Bifurcations

Let us consider the case where two of the parameters $a,\ b$ and c are varied – say along a curve in one of the parameter planes passing through a point where two of the eigenvalues of (13) are equal -1, while the remaining eigenvalue is of absolute value less than one. A natural question to ask for this codimension -2 parameter variation is, what are the properties of any flip bifurcations that may occur?

To see what flip possibilities there may be, it is instructive to first investigate the simple, uncoupled all-pioneer map

$$P(x_1,\ x_2,\ x_3) = (x_1 e^{a-x_1},\ x_2 e^{b-x_2},\ x_3 e^{c-x_3})$$

International Electronic Journal of Pure and Applied Mathematics – IEJPAM, Volume 1, No. 3 (2010)

with $a = b = 2$ and $0 < c < 2$. Let us fix c and vary a and b along the curve $b - a = 0$ in the a, b-plane, concentrating on a neighborhood of $(a,\ b) = (2,\ 2)$ in this plane. Owing to the fact that the system is uncoupled, Theorem 4.4 applied to each coordinate function yields the following characterization of the flip bifurcations at $x_* = (a = 2,\ b = 2,\ c)$: As a and b cross the value 2 in an increasing fashion along any smooth curve in the a, b-plane passing through $(2,\ 2)$, flip bifurcations occur. These bifurcations can be described as follows: In addition to the trivial, unstable 2-cycle at $(a,\ b,\ c)$ we have:

1. There are a pair of (nontrivial) stable 2-cycles; namely $\{(a+y_1^{(-)},\ b+y_2^{(-)},\ c),\ (a+y_1^{(+)},\ b+y_2^{(+)},\ c)\}$ and $\{(a+y_1^{(-)},\ b+y_2^{(+)},\ c),\ (a+y_1^{(+)},\ b+y_2^{(+)},\ c)\}$.

2. There are also two (nontrivial) stable 2-cycles; namely $\{(a+y_1^{(-)},\ b,\ c),\ (a+y_1^{(+)},\ b,\ c)\}$ and $\{(a,\ b+y_2^{(-)},\ c),\ (a,\ b+y_1^{(-)},\ c)\}$,

and in all cases the fixed point $(a,\ b,\ c)$ changes from an attractor to a repeller upon such a crossing of $(2,\ 2)$ in the a, b-plane.

As one might expect, our general hierarchical 3-dimensional system has analogous qualitative, codimension-2 flip bifurcation behavior. We summarize this in the following theorem, which we prove in Appendix.

Theorem 4.6. *Suppose that two of the eigenvalues of (13) at a fixed point $\hat{x}$ are equal to -1, while the remaining eigenvalue is less than one in absolute value. Let the parameters associated with the eigenvalues equal to -1 be varied across a smooth curve through the point in their coordinate plane so as to simultaneously increase the two parameters. Then just as in the uncoupled case above, in a neighborhood of the fixed point $\hat{x}$, $\hat{x}$ changes from an attractor to a repeller as the parameters pass through the bifurcation point, giving birth to four (nontrivial) 2-cycles; two of which are stable, while the other two are unstable.*

4.3. Codimension – Three Flip Bifurcations

To complete our analysis of flip bifurcations, we consider the case where $a,\ b$ and c are simultaneously varied past values where all of the eigenvalues of (13) are equal to -1. Again we take our cue from the uncoupled, all pioneer system; this time with $a = b = c = 2$, and $a,\ b$ and c simultaneously exceeding 2 along some curve in a, b, c-space passing through $(2,\ 2,\ 2)$. By analogy with our codimension-2 flip bifurcation investigation of (12), it is easy to see that for $a = 2+\mu_1,\ b = 2+\mu_2$ and $c = 2+\mu_3$ with $\mu_1,\ \mu_2,\ \mu_3 \geq 0$ sufficiently small, we have the following flip bifurcation properties: There are four stable 2-cycles; namely

$$\{(a+\phi^{(+)}(\sqrt{\mu_1}),\ b+\phi^{(+)}(\sqrt{\mu_2}),\ c+\phi^{(+)}(\sqrt{\mu_3})),$$
$$(a+\phi^{(-)}(\sqrt{\mu_1}),\ b+\phi^{(-)}(\sqrt{\mu_2}),\ c+\phi^{(-)}(\sqrt{\mu_3}))\},$$

International Electronic Journal of Pure and Applied Mathematics – IEJPAM, Volume 1, No. 3 (2010)

$$\{(a+\phi^{(+)}(\sqrt{\mu_1}),\ b+\phi^{(+)}(\sqrt{\mu_2}),\ c+\phi^{(-)}(\sqrt{\mu_3})),$$
$$(a+\phi^{(-)}(\sqrt{\mu_1}),\ b+\phi^{(-)}(\sqrt{\mu_2}),\ c+\phi^{(+)}(\sqrt{\mu_3}))\},$$
$$\{(a+\phi^{(+)}(\sqrt{\mu_1}),\ b+\phi^{(-)}(\sqrt{\mu_2}),\ c+\phi^{(+)}(\sqrt{\mu_3})),$$
$$(a+\phi^{(-)}(\sqrt{\mu_1}),\ b+\phi^{(+)}(\sqrt{\mu_2}),\ c+\phi^{(-)}(\sqrt{\mu_3}))\},$$

and

$$\{(a+\phi^{(+)}(\sqrt{\mu_1}),\ b+\phi^{(-)}(\sqrt{\mu_2}),\ c+\phi^{(-)}(\sqrt{\mu_3})),$$
$$(a+\phi^{(-)}(\sqrt{\mu_1}),\ b+\phi^{(+)}(\sqrt{\mu_2}),\ c+\phi^{(+)}(\sqrt{\mu_3}))\}.$$

Moreover, there are ten unstable 2-cycles, which are the fixed point $(a,\ b,\ c)$ and the nontrivial 2-cycles

$$\{(a+\phi^{(+)}(\sqrt{\mu_1}),\ b,\ c),\ (a+\phi^{(-)}(\sqrt{\mu_1}),\ b,\ c)\},$$
$$\{(a,\ b+\phi^{(+)}(\sqrt{\mu_2}),\ c),\ (a,\ b+\phi^{(-)}(\sqrt{\mu_2}),\ c)\},$$
$$\{(a,\ b,\ c+\phi^{(+)}(\sqrt{\mu_3})),\ (a,\ b,\ c+\phi^{(-)}(\sqrt{\mu_3}))\},$$

$$\{(a+\phi^{(+)}(\sqrt{\mu_1}),\ b+\phi^{(+)}(\sqrt{\mu_2}),\ c),\ (a+\phi^{(-)}(\sqrt{\mu_1}),\ b+\phi^{(-)}(\sqrt{\mu_2}),\ c)\},$$
$$\{(a+\phi^{(+)}(\sqrt{\mu_1}),\ b+\phi^{(-)}(\sqrt{\mu_2}),\ c),\ (a+\phi^{(-)}(\sqrt{\mu_1}),\ b+\phi^{(+)}(\sqrt{\mu_1}),\ c)\},$$
$$\{(a+\phi^{(+)}(\sqrt{\mu_1}),\ b,\ c+\phi^{(+)}(\sqrt{\mu_3})),\ (a+\phi^{(-)}(\sqrt{\mu_1}),\ b,\ c+\phi^{(-)}(\sqrt{\mu_3}))\},$$
$$\{(a+\phi^{(+)}(\sqrt{\mu_1}),\ b,\ c+\phi^{(-)}(\sqrt{\mu_3})),\ (a+\phi^{(-)}(\sqrt{\mu_1}),\ b,\ c+\phi^{(+)}(\sqrt{\mu_3}))\},$$
$$\{(a,\ b+\phi^{(+)}(\sqrt{\mu_2}),\ c+\phi^{(+)}(\sqrt{\mu_3})),\ (a,\ b+\phi^{(-)}(\sqrt{\mu_2}),\ c+\phi^{(-)}(\sqrt{\mu_3}))\},$$
$$\{(a,\ b+\phi^{(+)}(\sqrt{\mu_2}),\ c+\phi^{(-)}(\sqrt{\mu_3})),\ (a,\ b+\phi^{(-)}(\sqrt{\mu_2}),\ c+\phi^{(+)}(\sqrt{\mu_3}))\}.$$

In view of our analysis of codimension-2 flip bifurcations for our hierarchical map, it should come as no surprise that the qualitative behavior of the general case is the same as for the uncoupled system. More precisely, we have the following result that can be proved using the same techniques as in the codimension-1 and codimension-2 cases (albeit with many more detailed calculations), so that we omit the proof (cf. [9]).

Theorem 4.7. *Suppose that all three of the eigenvalues of (13) are equal to -1 at a fixed point $\hat{x}$ of F for a particular set of parameter values $(a,\ b,\ c) = (a_0,\ b_0,\ c_0)$ and consider $(a,\ b,\ c) = (a_0,\ b_0,\ c_0) + (\mu_1,\ \mu_2,\ \mu_3)$ for sufficiently small $\mu_1,\ \mu_2,\ \mu_3 \geq 0$, defining $\hat{x} = \hat{x}(a,b,c)$ and $x_* = \hat{x}(a,\ b,\ c)+(y_1,\ y_2,\ y_3)$. Then for $\mu_1,\ \mu_2,\ \mu_3 > 0$ sufficiently small, $F^2(x_*) = x_*$ has 27 solutions comprising a total of thirteen (non trivial) two-cycles of F near $\hat{x}(a_0,\ b_0,\ c_0)$ and the fixed point. These 2-cycles consist of four stable 2-cycles, and nine unstable 2-cycles; while the fixed point $\hat{x}$ is unstable. All of these 2-cycles depend analytically on $(\sqrt{\mu_1},\ \sqrt{\mu_2},\ \sqrt{\mu_2})$ for sufficiently small $\mu_1,\ \mu_2,\ \mu_3 \geq 0$, and shrink to $\hat{x}(a_0,\ b_0,\ c_0)$ as $\sqrt{\mu_1}+\sqrt{\mu_2}+\sqrt{\mu_3} \downarrow 0$.*

International Electronic Journal of Pure and Applied Mathematics – IEJPAM, Volume 1, No. 3 (2010)

5. Chaotic Dynamics

In this section we shall study chaotic regimes for our HPCM. Naturally, we shall take advantage of the h-principle to reduce the analysis to a 1-dimensional map in most cases, but we shall also have something to say about finding chaos in the complete higher dimensional system. "Perhaps" the most interesting behavior that one may observe in population dynamics is transition to chaotic regimes, possibly including strange chaotic attractors. From an ecologist's point of view, chaos plays an important role in predicting (or more accurately not being able to make long-time predictions about) the growth of plants in an ecosystem. If chaotic dynamics occurs, the behavior of the species can, besides being quite unpredictable to the point of appearing stochastic, be extremely complex and especially interesting. It appears from our simulations that our 3-dimensional all-climax discrete hierarchical model can exhibit chaotic dynamics, as shown in Figure 3 for the case where

$$F(x_1, x_2, x_3) = \left(x_1^2 e^{2.7-x_1}, x_2(x_1+x_2)e^{2.8-x_1-x_2}, x_3(x_1+x_2+x_3)e^{3-x_1-x_2-x_3}\right). \tag{14}$$

5.1. Three-Cycle Induced Chaos

We now proceed to prove that the one-dimensional pioneer case has a 3-cycle, which induces chaos in the HPCM if it has a pioneer coordinate function in accordance with the h-principle and [12], [21]. To demonstrate this, we consider the following all-pioneer version of the HPCM

$$\begin{aligned} F(x_1, x_2, x_3) &= (f_1(x_1), f_2(x_1, x_2), f_3(x_1, x_2, x_3)) \\ &:= \left(x_1 e^{a-x_1}, x_2 e^{b-\alpha x_1 - x_2}, x_3 e^{c-\beta x_1 - \gamma x_2 - x_3}\right), \end{aligned} \tag{15}$$

where $a,\ b,\ c > 0$ and $\alpha,\ \beta,\ \gamma > 0$. We restrict our demonstration to showing how chaos in the first coordinate map induced by the existence of a superstable 3-cycle for $x \to f_1(x) := xe^{a-x}$ generates a chaotic orbit for the whole system. Note first that $f_1(0) = 0$ and $f_1(x) \downarrow 0$ as $x \uparrow \infty$. The fixed points are $x = 0$ and $x = a$. To see if these are stable, we compute

$$f_1' = (1-x)e^{a-x}.$$

Hence,

$$\begin{aligned} &f_1'(0) = e^a > 1 \ \Rightarrow\ 0 \text{ is an unstable fixed point,} \\ &f_1'(a) = (1-a) \ \Rightarrow\ x = a \text{ is stable if } 0 < a < 2 \text{ and unstable if } a > 2. \end{aligned}$$

Let us find the maximum and maximizer for this function. As

$$f_1' = (1-x)e^{a-x} = 0 \ \Rightarrow\ x = 1,$$

International Electronic Journal of Pure and Applied Mathematics – IEJPAM, Volume 1, No. 3 (2010)

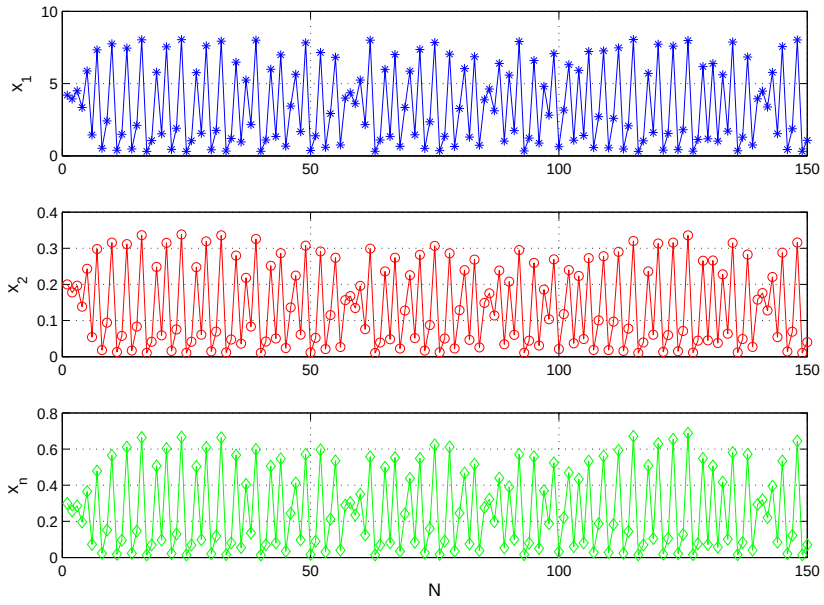

Figure 3: Apparent chaotic behavior for the all climax discrete hierarchical case with $a = 2.7$, $b = 2.8$, $c = 3.0$. The interspecies and intraspecies interaction coefficients are 1

the maximizer is $x = 1$ and the maximum is $f_1(1) = e^{a-1}$. A graph of f_1 is sketched in Figure 4 (for $a > 1$).

We now find an a having a superstable 3-cycle including the maximizer where $f_1' = 0$ ($\Rightarrow$ superstable). Such a cycle is illustrated with the cobweb map shown in Figure 5. We see from the cobweb map that

$$x_{(0)} = 1 \ \rightarrow \ x_{(1)} := f_1(x_{(0)}) = e^{a-1} \rightarrow \ x_{(2)} := f_1(x_{(1)}) = e^{a-1}\exp(a - e^{a-1})$$
$$\rightarrow \ x_{(0)} := f_1(x_{(2)}) = e^{a-1}\exp(a - e^{a-1})\exp[a - (e^{a-1}\exp(a - e^{a-1}))].$$

Accordingly a must satisfy the equation

$$\Delta(a) := 3a - 1 - e^{a-1}[1 + \exp(a - e^{a-1})] = 0. \tag{16}$$

Clearly, $a = 1$ is a solution, but this just produces a degenerate 3-cycle comprised only of the fixed point $x = a$. We seek another solution with $a = a_* > 2$. Note that a simple computation shows that

$$\Delta(3) = 8 - e^2[1 + \exp(3 - e^2)] \cong 0.51923 > 0$$

International Electronic Journal of Pure and Applied Mathematics – IEJPAM, Volume 1, No. 3 (2010)

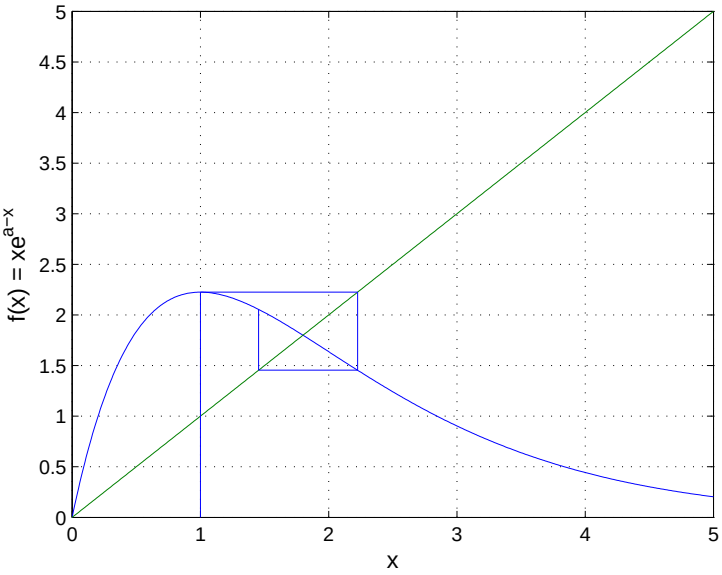

Figure 4: A cobweb map for pioneer species with the positive parameter $a = 1.8$

and

$$\Delta(4) = 11 - e^3[1 + \exp(4 - e^3)] \cong -9.08554 < 0.$$

Thus the desired solution of (16) lies between 3 and 4. Using the bisection method [10], we compute that

$$a_* \cong 3.1167,$$

and conclude that $f(x) := xe^{a-x}$ has a superstable 3-cycle comprised of the points $\{1,\ e^{a_*-1},\ e^{a_*-1}\exp(a_* - e^{a_*-1})\}$.

Returning to the original system (15), let us first consider the case where, $\alpha,\ \beta,\ \gamma = 0$, so we have the uncoupled system

$$\begin{aligned} x_1(n+1) &= x_1(n)e^{a_*-x_1(n)}, \\ x_2(n+1) &= x_2(n)e^{b-x_2(n)}, \\ x_3(n+1) &= x_3(n)e^{c-x_3(n)}. \end{aligned} \tag{17}$$

If we set $b = c = 1.5$, then it is clear from the above that

$$\{(1,\ b,\ c),\ (e^{a_*-1},\ b,\ c),\ (e^{a_*-1}\exp(a_* - e^{a_*-1}),\ b,\ c)\}$$

International Electronic Journal of Pure and Applied Mathematics – IEJPAM, Volume 1, No. 3 (2010)

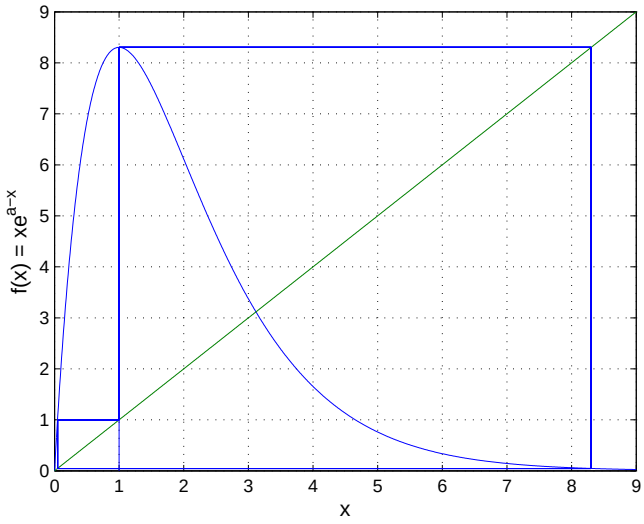

(a) A superstable 3-cycle

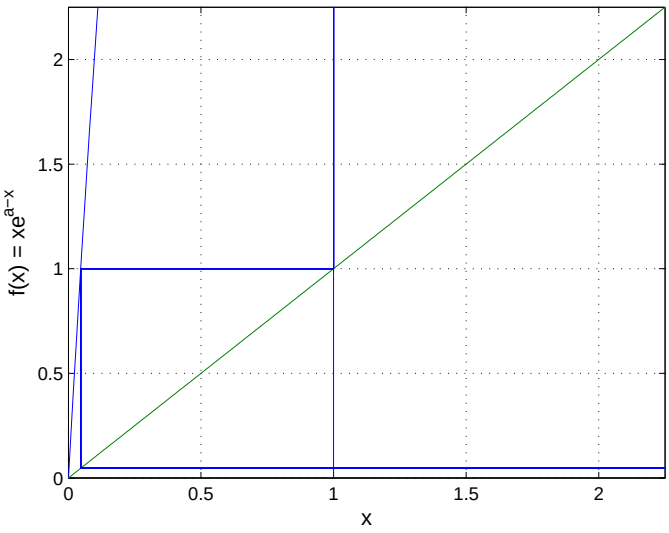

(b) Zoomed version of Figure 5(a)

Figure 5: Cobweb map for pioneer species with parameters $a = 3.1167$ and $c_{11} = 1$

is a stable 3-cycle of (15). We want to consider some coupling, but not to the extent that it perturbs this stable 3-cycle by much. Therefore, we consider the following

International Electronic Journal of Pure and Applied Mathematics – IEJPAM, Volume 1, No. 3 (2010)

special case:

$$\begin{aligned} x_1(n+1) &= x_1(n)e^{a_*-x_1(n)}, \\ x_2(n+1) &= x_2(n)e^{1.5-0.3x_1(n)-x_2(n)}, \\ x_3(n+1) &= x_3(n)e^{1.5-0.3x_1(n)-0.3x_2(n)-x_3(n)}. \end{aligned} \tag{18}$$

It follows from the h-principle that this has a 3-cycle of the form

$$\{(1,\ x_2^{(0)},\ x_3^{(0)}),\ (e^{a_*-1},\ x_2^{(1)},\ x_3^{(1)}),\ (e^{a_*-1}\exp(a_*-e^{a_*-1}),\ x_2^{(2)},\ x_3^{(2)})\}.$$

A bit of straightforward analysis of the corresponding solution of $F^3(\boldsymbol{x}) = \boldsymbol{x}$ (backed up by numerical simulations) is all that it takes to show that we can choose $x_2^{(0)}$ and $x_3^{(0)}$ close to $b = c = 1.5$ in a way that $x_2^{(1)}$, $x_3^{(1)}$, $x_2^{(2)}$ and $x_3^{(2)}$ are also close to 1.5, and that the 3-cycle is stable. Of course, period three does not necessarily imply chaos in more than one dimension, but we do obtain chaos since the 1-dimensional first coordinate has a (superstable) 3-cycle. The difference between orbits starting near (but not on) the 3-cycles of these two systems is that for (17) only the iterates of the x_1 coordinate are chaotic, while in the case of (18) all of the coordinate iterates evolve chaotically.

The existence of a chaotic orbit is additionally supported by the bifurcation diagrams in Figs. 6 and 7 and computation of the Lyapunov exponent of an orbit for the first coordinate map starting near $x_1 = 1$ shown in Figure 8. These observations and calculations also apply to the cases when the second and third coordinate maps have chaotic orbits, and to a more general HPCM comprised of any permutation of pioneer and climax coordinate maps.

5.2. Period-Doubling Route to Chaos

It follows from the h-principle that if any pioneer or climax coordinate map in our HPCM exhibits the well-known (for unimodal maps) period-doubling route to chaos, so does the entire system. The bifurcation diagrams in Figs. 6 and 7, and Figure 9 show the behavior of a pioneer and climax species, respectively, for a range of values of a. One sees the expected appearance of chaos beyond the limit of a period-doubling cascade in each case.

For the pioneer map $f(x) = xe^{a-x}$, as a increases from 0 we have a single stable fixed point at $\hat{x} = a$. But at $a \cong 1.985$, the fixed point becomes unstable and bifurcates into a stable 2-cycle comprising points just to the right and left of a via a flip bifurcation. This two-cycle further becomes unstable and bifurcates into a stable 4-cycle and these period-doubling bifurcations continue with increasing a, generating a period-doubling cascade that reaches a limit at $a \cong 2.69$. There is a period-3 window at $a \cong 3.105$, showing the existence of chaos for a single species owing to the work of Sharkovski [21] and Li and Yorke [12]. Note that beyond $a \cong 8.575$ it appears

International Electronic Journal of Pure and Applied Mathematics – IEJPAM, Volume 1, No. 3 (2010)

that the bifurcation diagram degenerates to zero, indicating an almost complete lack of stable invariant subsets. The Lyapunov exponent λ graph in Figure 8 confirms these observations, indicating the existence of chaotic orbits (since $\lambda > 0$) for most values exceeding the period-doubling limit. We also see a very strong positive jump in the exponent at $a \cong 7.67$ followed by monotone increasing values, which we shall have more to say about shortly.

In the case of a climax coordinate map $g(x) = x^2 e^{a-x}$, there is an analogous period-doubling cascade leading to chaos depicted in the bifurcation diagram in Figure 9. However, in this case $x = 0$ remains superstable for all a, and there is a positive stable fixed point for $1 < a < 3 - \ln 3$. As a increases just beyond $3 - \ln 3$, the fixed point becomes unstable and gives birth to a stable 2-cycle, which becomes unstable at $a \cong 2.43$ and generates a stable 4-cycle. This process continues and generates a period-doubling cascade with a limit of $a \cong 2.45$, and one can expect the existence of chaotic regimes beyond this parameter value. There is a period-3 window at $a \cong 2.62$, which implies chaos for this 1-dimensional map (and the entire HPCM owing to the h-principle). The bifurcation diagram collapses to the superstable attractor at the origin for $a \cong 2.97$, and it is not difficult to show (in fact it follows directly from our shift map construction in the sequel) that the origin is an almost global attractor for $a > 2.97$, in the sense that it attracts all orbits except those starting on a set of (Lebesgue) measure zero. The conclusions concerning the existence of chaotic orbits for the climax map are also supported by the graph of Lyapunov exponents in Figure 10.

5.3. Shift Map Chaos

The existence of chaotic orbits for a climax map can also be proved using a fairly standard construction that demonstrating that there is a compact invariant set on which g acts like a shift map (cf. [1], [5], [7], [15], [26]). Consider the 1-dimensional climax species map

$$g(x) := x^2 e^{a-x}.$$

Numerical experiments indicate that we can apply the standard Cantor set argument to prove existence of chaos when $a \geq 2.98$, so we will now focus our attention on the specific map

$$g(x) = x^2 e^{2.98-x} \tag{19}$$

having the graph shown in Figure 11. The fixed points of g are 0, and approximately 0.0536 and 4.4795. An $x \in I = [0.0536,\ 10.6436]$ has two types of orbits: one which directly or eventually goes to the origin (extinction or saturation of population leading to extinction) and a second which does not converge to the origin (flourishing). We are interested in the second case. So, we shall remove all the subintervals from I which give rise to orbits converging to the origin and then observe the behavior of (19) on the remainder of I.

International Electronic Journal of Pure and Applied Mathematics – IEJPAM, Volume 1, No. 3 (2010)

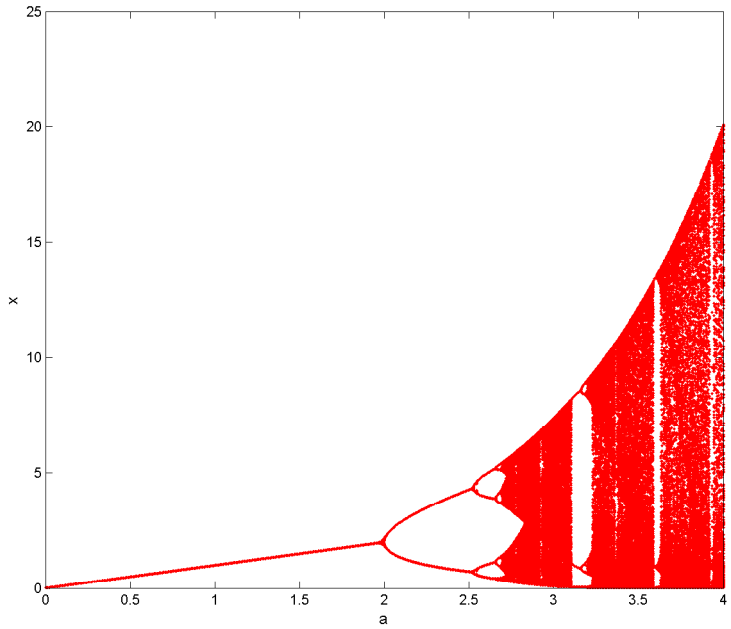

Figure 6: Bifurcation diagram for a pioneer species. Here the parameter a varies from 0-4

Let us denote the set of all points in I whose iterates do not converge to the origin by Λ. We clearly have the subinterval $I_0 = (1.54,\ 2.55)$ whose points ultimately go to the origin. Next we have two more subintervals: $I_1^{(-)} = (0.32,\ 0.45)$ on the left of I_0 and $I_1^{(+)} = (5.42,\ 6.19)$ on the right of I_0. They represent $g^{-1}(I_0)$, the preimage of I_0. So the points in $I_1^{(-)}$, $I_1^{(+)}$ are first mapped to I_0 and then they go to the origin. We will remove these three subintervals from I. Now we repeat this procedure, i.e. to find the preimage of $I_1^{(-)}$ which is $I_2^{(-)} = (0.13,\ 0.16) \cup (0.77,\ 0.86)$ and of $I_1^{(+)}$ which is $I_2^{(+)} = (3.85,\ 4.12) \cup (7.91,\ 8.36)$. At any stage k of this process, we find 2^k subintervals whose forward iterates under g converge to the origin, and are to be removed from I. This construction is illustrated in Figure 11.

This process of removal generates a compact, 2-component Cantor set (of measure zero) defined as

$$\Lambda := I \setminus \left(I_0 \cup \left(\bigcup_{k=1}^{\infty} I_k^{(\pm)} \right) \right).$$

It is clear from the construction that $g(\Lambda) \subset \Lambda$, so this Cantor set is invariant.

International Electronic Journal of Pure and Applied Mathematics – IEJPAM, Volume 1, No. 3 (2010)

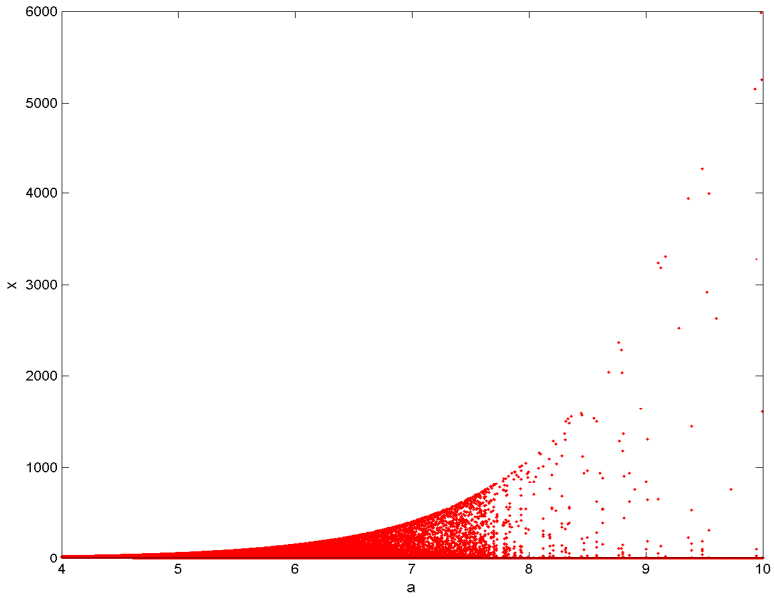

Figure 7: Bifurcation diagram for a pioneer species. Here the parameter a varies from 4-10

Each $x \in \Lambda$ can be identified with a binary sequence as follows:

$$x \leftrightarrow .a_0a_1a_2\ldots$$

where,

$$a_k := \begin{cases} 0, & g^k(x) \in J_0; \\ 1, & g^k(x) \in J_1, \end{cases}$$

where $J_0 = [0.0536, 1.54)$ and $J_1 = (2.55, 10.6436]$. The fixed points 0.0536 and 4.4 795 naturally belong to J_0 and J_1, respectively, since the iterates of these points are fixed. In terms of the identification (homeomorphism), the positive fixed points are identified with the points $.0000\ldots$ and $.1111\ldots$ respectively. Note here that this also shows that the set of initial points whose orbits do not converge to zero has measure zero.

The restriction $g_{|\Lambda}$ is, by a standard argument (see, e.g. [1], [5], [15], [26]) that follows right from its definition, topologically conjugate to the shift map $\sigma : S \to S$, defined in the space of binary sequences of the form $.a_0a_1a_2,\ldots$ as

$$\sigma(.a_0a_1a_2\ldots) := .a_1a_2a_3\ldots$$

International Electronic Journal of Pure and Applied Mathematics – IEJPAM, Volume 1, No. 3 (2010)

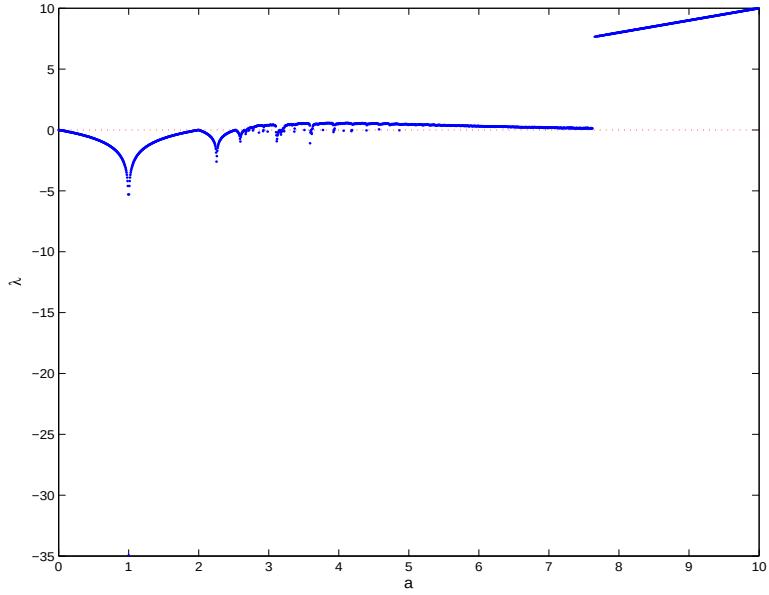

Figure 8: Lyapunov exponents for a pioneer species

Therefore, g is chaotic on Λ and has such features as periodic orbits of all periods and a dense orbit. Accordingly the h-principle implies the existence of chaotic orbits for the HPCM with a climax coordinate function having a sufficiently large growth rate.

5.4. Small Scale Strange Attractor Like Pioneer Behavior

Let us look a little more closely at the dynamics of both pioneer and climax coordinate maps for larger growth rates. Denote the pioneer and climax maps by $f_a(x) := xe^{a-x}$ and $g_a(x) := x^2e^{a-x}$ respectively, where the subscript a is included to emphasize the dependence on this parameter. We have already essentially taken care of this for g_a: Figure 9 shows that for $a > 2.97$ the bifurcation diagram collapses to a thickened x-axis, and Figure 10 indicates the existence of chaotic orbits. But this follows from our discussion in the preceding subsection, where we showed that for such parameter values $g_a^n(x)$ converges almost everywhere to the superstable attractor at the origin, and the complement Λ of this attraction set is an unstable compact, invariant, 2-component Cantor set on which g_a acts like a shift map.

The bifurcation diagrams Figs. 6 and 7 and Lyapunov exponent graph Figure 8 for f_a exhibit analogous behavior, except that this occurs for $a > 8.575$ and the

International Electronic Journal of Pure and Applied Mathematics – IEJPAM, Volume 1, No. 3 (2010)

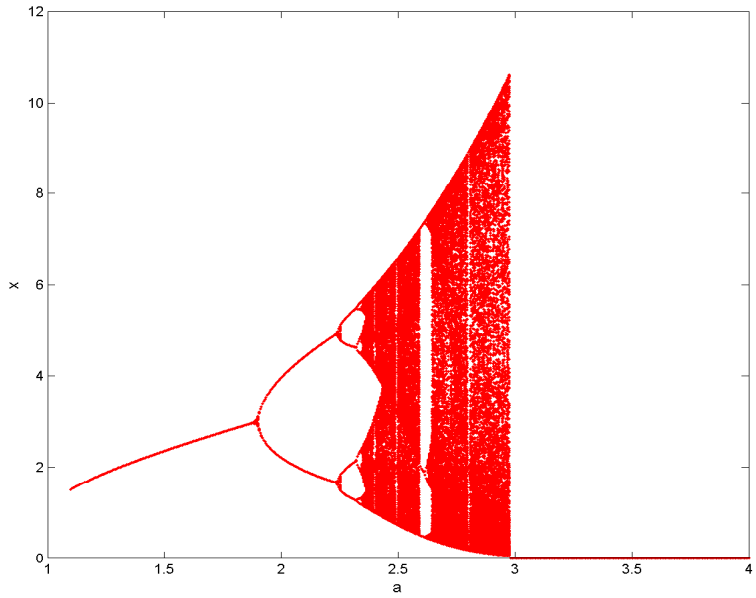

Figure 9: Bifurcation diagram for a climax species. Here the parameter a varies from 1.1-4

Lyapunov exponent appears to be quite a bit more positive for the pioneer map. For such large values of a, the fixed point at the origin is strongly repelling rather than contracting as in the case of g_a. Consequently, in spite of the similarities in the bifurcation diagrams and Lyapunov exponent graphs for f_a and g_a, their dynamics cannot be the same. It remains only to characterize the large growth rate dynamics for the pioneer map. What we shall show is that given any small positive ϵ, the orbit of almost every point visits the interval $I_\epsilon := [0, \epsilon)$ infinitely often and this interval contains an invariant Cantor set for some iterate $f_a^{N(\epsilon)}$ on which it behaves like a shift map (i.e. f_a is a subshift). Consequently, there is something akin to a strange attractor in any small neighborhood of the origin, except almost all orbits only come close to the "attractor" infinitely often instead of converging to it. This may explain the thickening of the unstable origin in the bifurcation diagram and rapid increase in the Lyapunov exponent for large values of a.

To verify this behavior, first recall that the maximum, e^{a-1}, of f_a occurs at $x = 1$, so $f_a(\mathbf{R}_+) = [0, e^{a-1}]$. The image of the right end point of this interval is $f_a^2(1) = \exp\left(2a - 1 - e^{a-1}\right)$. It follows by a simple calculation that given any $0 < \epsilon \ll 1$, $f_a^2(1) < \epsilon$ whenever $a > 1 + \ln\left(\ln(\epsilon^{-2})\right)$ and $a \geq 4$. Now fix an a

International Electronic Journal of Pure and Applied Mathematics – IEJPAM, Volume 1, No. 3 (2010)

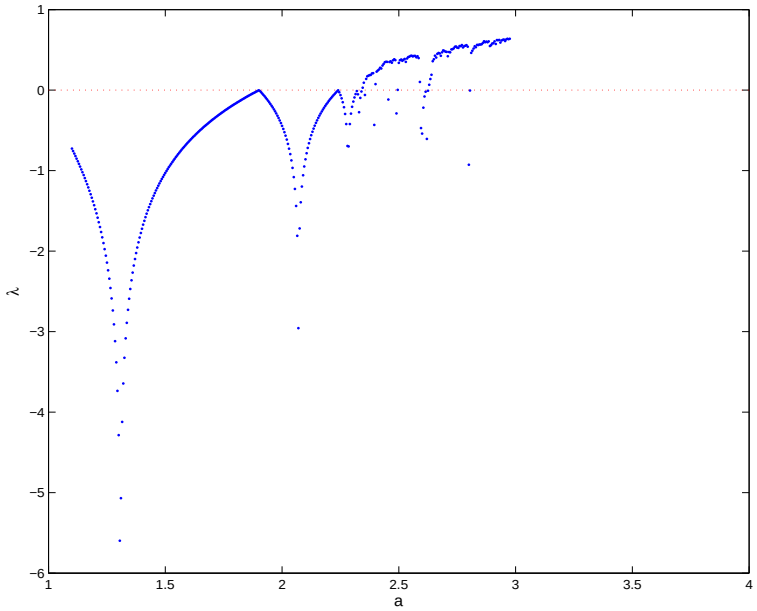

Figure 10: Lyapunov exponents for a climax species

satisfying these inequalities, and note that a simple calculation shows for example that $f_a^2(1) < 1.0 \times 10^{-6}$ when $a > 8.575$. Define

$$\Theta(a) := \{x \in \mathbf{R}_+ : f_a^n(x) \in I_\epsilon \text{ for infinitely many nonnegative integers } n\}.$$

The set $\Theta(a)$ is f_a-invariant by its very definition, and a straightforward modification of the Cantor set construction for the climax map above along with some basic measure theoretic results can be used to show that its complement has measure zero. Observe that the complement of $\Theta(a)$, which we denote as $\Xi(a)$, also is invariant.

It is easy to see, by decreasing ϵ if necessary, that we can choose $N = N(\epsilon) > 2$ so large that the (restricted) function $\varphi := f_{a|I_\epsilon}^N$ has the following properties: (1) It is unimodal. (2) φ has just one maximizer $x_m > 0$ on I_ϵ at which φ is equal to e^{a-1} and for which $\varphi'(x)$ is positive (negative) when $0 \le x < x_m$ ($x_m < x < \epsilon$). (3) It has precisely two fixed points: one at zero and the other at x_r, where $x_m < x_r < \epsilon$. (4) $x_r < \varphi(x_m) = e^{a-1}$. In all, the graph of φ is essentially a strongly horizontally contracted version of the graph of f_a on $[0, e^{a-1}]$. These properties can readily be seen to imply that there exists b and an open subinterval U of I_ϵ such that $x_r < b < \epsilon$, $x_m \in U$ and $\varphi(U) \cap [0, b] = \varnothing$. In a manner analogous to that in the

International Electronic Journal of Pure and Applied Mathematics – IEJPAM, Volume 1, No. 3 (2010)

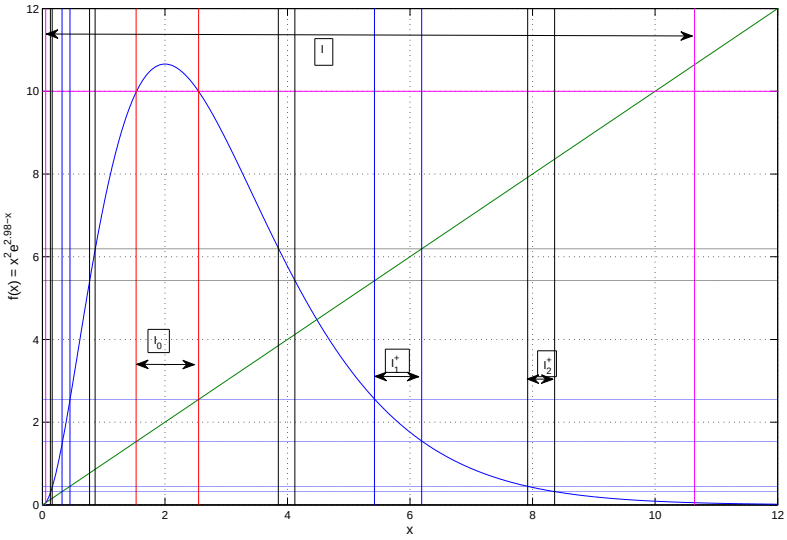

Figure 11: The formation of the Cantor set

preceding subsection, we define

$$\Delta := [0, b] \setminus \bigcup_{n=0}^{\infty} \left(\varphi^{-n}(U) \cap [0, b]\right),$$

which yields a compact, φ-invariant, 2-component Cantor set on which the restriction $\varphi_{|\Delta}$ is conjugate to a shift map, and is therefore chaotic – and very strongly so due to the high strength of repulsion of Δ. These properties certainly provide a plausible explanation for the behavior of the bifurcation diagrams and Lyapunov exponent graphs of a pioneer map for large values of a.

The properties of the fractal invariant set Δ in any given I_ϵ show that although it is repelling, it has a small neighborhood - namely I_ϵ – that intermittently attracts almost all points on $\mathbf{R}_+$; suggesting that it be called a *strange persistent set*. And even though this set is not stable, its existence in any neighborhood of the origin together with the bifurcation diagram results, suggests that this effect may actually be observable in real ecological systems where it would manifest itself as chaotic small scale behavior of one or more pioneer species.

5.5. Higher Dimensional Horseshoe Induced Chaos

As a final means of identifying chaotic behavior in our HPCM, we shall very briefly describe a higher dimensional horseshoe method. The idea is to locate connected

International Electronic Journal of Pure and Applied Mathematics – IEJPAM, Volume 1, No. 3 (2010)

m-dimensional polyhedron P in $\mathbf{R}_+^m$ for which $F(P)$ exhibits the basic properties of compression, stretching, folding and intersection with P in two or more components, whereupon we can mimic the standard 2-dimensional construction in order to detect the existence of transverse homoclinic points leading to chaos. To illustrate this, we shall continue to restrict our attention to $m = 3$, and investigate the following all-climax map:

Example 5.1. Consider the map $F : \mathbf{R}_+^3 \to \mathbf{R}_+^3$ defined as in (14). Then with some computational help that for example produces Figure 3 showing the coordinate "time series" indicating chaotic motion, we identify the tetrahedron P with vertices at $(0.01, 0.01, 0.25)$, $(0.01, 0.01, 0.27)$, $(0.01, 6, 0.3)$, and $(8, 0.01, 0.3)$ as a promising choice. Computer graphics can be used to show that $F(P)$ has the proper horseshoe properties with respect to P, with $F(P)$ piercing P twice in disjoint subsets, and this can be proved by direct calculation and estimation of the image of P. Thus we have an alternate means of proving chaos, but one that requires some rather painstaking analysis.

6. Concluding Remarks

We formulated a novel (but natural) extension of an hierarchical discrete dynamical model for the evolution of pioneer and complex species – one that has proven to be quite effective in predicting the behavior of just two such species. After a thorough analysis of the basic dynamical properties of this system, which highlighted the fact that the hierarchical nature of the system renders many dynamical considerations essentially one-dimensional (the h-principle), we turned our attention to periodic, bifurcation and chaotic phenomena for the model. For example, we showed that although the system cannot exhibit Hopf bifurcation, it does have a very rich variety of flip bifurcation dynamics. Lastly, we made extensive use of the h-principle, techniques for identifying chaos in one-dimensional maps and a geometric horseshoe based procedure to prove the existence of chaos for a wide range of system parameter values. In the process, we introduced the notion of a strange persistent set to characterize certain behavior of pioneer coordinate maps in the system for large population growth rates, which although unstable may prove to be observable in real pioneer-climax systems.

Naturally, there is much work left to be done on higher dimensional pioneer-climax systems. For one, we plan to investigate the existence of true strange attractors in discrete dynamical models (in addition to the strange persistent sets identified here). These strange attractors would, by their very nature, be readily observable by ecologists, and may prove a very good starting point for seeking experimental data that confirms or confutes the predictions of our model, thereby possibly beginning effective collaboration with ecologists in particular, and population biologists in general.

International Electronic Journal of Pure and Applied Mathematics – IEJPAM, Volume 1, No. 3 (2010)

Acknowledgments

A portion of this paper was taken from the dissertation of the first author, completed in partial fulfillment of the requirements for the degree of Doctor of Philosophy in the Mathematical Sciences at the New Jersey Institute of Technology.

References

[1] D.K. Arrowsmith, C.M. Place, *Dynamical Systems: Differential Equations, Maps and Chaotic Behaviour*, Chapman and Hall, London (1992).

[2] J. Best, C. Castillo-Chavez, A.-A. Yakubu, Hierarchical competition in discrete time models with dispersal, *Fields Institute Communications*, **36** (2004), 59-86.

[3] J.E. Franke, A.-A. Yakubu, Exclusion principle for density-dependent discrete pioneer-climax models, *J. Math. Anal. Appl.*, **187** (1994), 1019-1046.

[4] J.E. Franke, A.-A. Yakubu, Pioneer exclusion in a one-hump discrete pioneer-climax competitive system, *J. Math. Biol.*, **32** (1994), 771-787.

[5] J. Guckenheimer, P. Holmes, *Nonlinear Oscillations, Dynamical Systems and Bifurcations of Vector Fields*, Springer-Verlag, New York (1983).

[6] M.P. Hassell, M.N. Comins, Discrete time models for two-species competition, *Theoret. Population Biol.*, **9** (1976), 202-221.

[7] M.W. Hirsch, S. Smale, R.L. Devaney, *Differential Equations, Dynamical Systems, and an Introduction to Chaos*, Elsevier Academic Press (2004).

[8] G. Jegan, G. Ramesh, K. Muthuchelian, Resprouting of Pioneer and Climax Species in the Pachakumachi Hills, Cumbum Valley, Western Ghats, India, *Ethnobotanical Leaflets*, **12** (2008), 343-347.

[9] Y. Joshi, *Discrete Dynamical Population Models: Higher Dimensional Pioneer-Climax Models*, Ph.D. Thesis, New Jersey Institute of Technology (2009).

[10] A. Kendall, *Introduction to Numerical Analysis*, Wiley, New York (1989).

[11] M.V. Kuijk, *Forest Regeneration and Restoration in Vietnam*, Ph.D. Thesis, Utrecht University (2008).

[12] Y.T. Li, J.A. Yorke, Period three implies chaos, *Am. Math. Month.*, **82** (1975), 985-992.

[13] D. Raaimakers, R.G.A. Boot, R. Dijkstra, S. Pot, T. Pons, Photosynthetic rates in relation to leaf phosphorus content in pioneer versus climax tropical rainforest trees, *Oecologia*, **12** (1995), 120-125.

[14] D. Raaimakers, H. Lambers, Response to phosphorus supply of tropical tree seedlings: a comparison between a pioneer species Tapirira obtusa and a climax species Lecythis corrugata, *Netv PhytoL*, **132** (1996), 97-102.

[15] C. Robinson, *Dynamical Systems: Stability, Symbolic Dynamics, and Chaos*, CRC Press Inc., Boca Raton (1995).

[16] J.F. Selgrade, Planting and harvesting for pioneer-climax models, *Rocky Mountain J. Math.*, **24** (1994), 293-310.

[17] J.F. Selgrade, G. Namkoong, Stable periodic behavior in a pioneer-climax model, *Nat. Resour. Model*, **4** (1990), 215-227.

[18] J.F. Selgrade, G. Namkoong, Population interactions with growth rates dependent on weighted densities, *Differential Equation Models in Biology, Epidemiology and Ecology, Lecture Notes in Biomath.*, **92** (1991), 247-256.

[19] J.F. Selgrade, J.H. Roberds, Lumped-density population models of pioneer-climax type and stability analysis of Hopf bifurcations, *Math. Biosci.*, **135** (1996), 1-21.

[20] J.F. Selgrade, J.H. Roberds, Period-doubling bifurcations for systems of difference equations and applications to models in population biology, *Nonlin. Anal.: Theory, Methods and Applications*, **29** (1997), 185-199.

[21] A.N. Sharkovski, Co-existence of the cycles of a continuous mapping of the line into itself, *Ukrainian Math. Z.*, **16** (1964), 61-71.

[22] M. Silvestrini, I.F.M. Válio, E.A. de. Mattos, Photosynthesis and carbon gain under contrasting light levels in seedlings of a pioneer and a climax tree from a Brazilian semideciduous tropical forest, *Rev. Bras. Bot.*, **30** (2007), 463-474.

[23] S. Sumner, *Dynamical Systems Associated with Pioneer-Climax Models*, Ph.D. Thesis, North Carolina State University (1992).

[24] S. Sumner, Hopf bifurcation in pioneer-climax competing species models, *Math. Biosci.*, **137** (1996), 1-24.

[25] Wikipedia, Lambert W function — Wikipedia, The Free Encyclopedia (2009), http://en.wikipedia.org/w/index.php?title=Lambert_W_function&oldid=306160

[26] S. Wiggins, *Introduction to Applied Nonlinear Dynamical Systems and Chaos*, Springer, New York (2003).

A. Appendix

We now give detailed proofs of Theorems 4.5 and 4.6.

A.1. Proof of Theorem on Codimension-1 Flip Bifurcations

For simplicity, we consider only the all-pioneer case, noting that all other combinations of pioneer and climax coordinate functions (with other interaction coefficients) can be dealt with analogously:

$$\begin{aligned} F(x) &= (f_1(x_1;\ a),\ f_2(x_1,\ x_2; b),\ f_3(x_1,\ x_2,\ x_3;\ c)) \\ &= (x_1 e^{a-x_1},\ x_2 e^{b-x_1-x_2},\ x_3 e^{c-x_1-x_2-x_3}). \end{aligned} \tag{20}$$

The fixed point in question must be $\hat{x} = (a,\ b-a,\ c-b)$. If it is λ_1 that equals -1, with associated $v = a$, the proof follows directly from the one-dimensional result in Theorem 4.4. If $\lambda_2 = -1$, or $\lambda_3 = -1$ with associated parameters b or c, respectively, the proof – in keeping with the h-principle – is only slightly more difficult. We consider only $\lambda_2 = -1$, since the proof for $\lambda_3 = -1$ is virtually the same. In this case, we see from (20) that the eigenvalues of $F'(\hat{x})$ are $-1 < \lambda_1 = 1 - a < 1,\ \lambda_2 = 1 - (b-a) = -1$ and $-1 < \lambda_3 = 1 - (c-b) < 1$. Now we fix a and vary b slightly while keeping c fixed and maintaining $-1 < 1 - (c-b) < 1$. Observe that

$$\begin{aligned} F^2(\boldsymbol{x}) &= F(F(\boldsymbol{x})) \\ &= (f_1(f_1(x_1)),\ f_2(f_1(x_1),\ f_2(x_1,\ x_2)),\ f_3(f_1(x_1), f_2(x_1,x_2), f_3(x_1,x_2,x_3))) \\ &= (x_1 \exp[2a - x_1(1+e^{a-x_1})],\ x_2 \exp[2b - x_1(1+e^{a-x_1}) - x_2(1+e^{b-x_1-x_2})], \\ &\quad x_3 \exp[2c - x_1(1+e^{a-x_1}) - x_2(1+e^{b-x_1-x_2}) - x_3(1+e^{c-x_1-x_2-x_3})]) \end{aligned} \tag{21}$$

and it is easy to see that $F^2(\hat{\boldsymbol{x}}) = F^2(a,\ b-a,\ c-b) = \hat{\boldsymbol{x}}$, so naturally $\hat{\boldsymbol{x}}$ is also a fixed point of F^2. To find the bifurcation in the x_2 coordinate, we set $v = b = a + 2 + \mu = v_* + \mu$, $x_2 = (b-a) + y_2 = 2 + \mu + y_2$ and $x_3 = c - b + y_3$. We want to find fixed points $\boldsymbol{x}_* = \hat{\boldsymbol{x}} + (0,\ y_2,\ y_3)$ of F^2 near $\hat{\boldsymbol{x}}$ for sufficiently small $\mu \geq 0$. It follows from (21) that $\boldsymbol{x}_*$ must satisfy the equations

$$\begin{aligned} 2(2+\mu) - (2+\mu+y_2)(1+e^{-y_2}) &= 0, \\ 2(c-a) - (b-a+y_2)(1+e^{-y_2}) - (c-b+y_3)(1+e^{-y_2-y_3}) &= 0. \end{aligned} \tag{22}$$

We see from the proof of Theorem 4.4 that the first of the above equations has in addition to $y_2 = 0$ a pair of nonzero solutions $y_2^{(-)} = -\sqrt{\mu}[\sqrt{6} + O(\mu)] \leq 0 \leq y_2^{(+)} =$

International Electronic Journal of Pure and Applied Mathematics – IEJPAM, Volume 1, No. 3 (2010)

$\sqrt{\mu}[\sqrt{6}+O(\mu)]$ for all sufficiently small $\mu \geq 0$. Upon substituting either of these in the second of equations (22), and taking note of the first equation, we obtain

$$\psi(y_3,\ \mu) := 2(c-b) - (c-b+y_3)(1+e^{-y_2^{(\pm)}(\sqrt{\mu})-y_3}) = 0.$$

We compute that $\frac{d\psi}{dy_3}(0,\ \mu) = -1 + [(c-b)-1]e^{-y_2^{(\pm)}(\sqrt{\mu})}$, whereupon it follows from $-1 < \lambda_3 = 1-(c-b) < 1$ that this derivative is not zero for all sufficiently small μ. Hence, we infer from the implicit function theorem that (22) has a unique solution $y_3^{(\pm)} = y_3^{(\pm)}(\mu)$ going to zero with μ, and $y_3(\mu)$ is actually a smooth function of $y_2(\mu)$, which is a smooth function of $\sqrt{\mu}$. Collecting all of the above properties, we see that

$$x_*^{(+)} = (a,\ b-a+y_2^{(+)},\ c-b+y_3^{(+)}),$$
$$x_*^{(-)} = F(x_*^{(+)}) = (a,\ b-a+y_2^{(-)}, c-b+y_3^{(-)})$$

is a 2-cycle of F in a neighborhood of the fixed point $\hat{x} = (a,\ b-a,\ c-b)$ for $b = a+2+\mu$ varying and the parameters a and c fixed. In addition, it is straightforward to show that $||\hat{x}-x_*|| = O(\sqrt{\mu})$ and that the eigenvalues of $F^{2\prime}(x_*^{(-)}) =$ eigenvalues of $F^{2\prime}(x_*^{(+)})$ all have absolute value less than 1, so $\{x_*,\ F(x_*)\}$ is a stable 2-cycle. As it is clear that the fixed point x_* is unstable (in the x_2 direction) for all sufficiently small $\mu > 0$, the proof is complete.

A.2. Proof of Theorem on Codimension-2 Flip Bifurcations

Once again, we shall give the proof only for the all-pioneer system (20), and here we shall only consider the case where $\lambda_1 = 1-a = \lambda_2 = 1-(b-a) = -1$, and $-1 < \lambda_3 = 1-(c-b) < 1$. A proof for the most general case, which we leave to the reader can be based on the argument that follows, with only minor modifications. We simply extend the methods of proof of Theorems 4.4 and 4.5. Denote the fixed point of F as $\hat{x} := (a,\ b-a,\ c-b)$, and set $a = 2+\mu$ and $b = a+2+\nu = 4+\mu+\nu$, where $\mu,\ \nu \geq 0$ are sufficiently small. Define $x_* = \hat{x} + (y_1,\ y_2,\ y_3) = (2+\mu+\nu,\ 2+\nu+y_2,\ c-(4+\mu+\nu)+y_3)$, which denotes solutions of $F^2(x_*) = x_*$ for $\mu, \nu \geq 0$ sufficiently small, and the $y_1,\ y_2,\ y_3$ are correspondingly small coordinate increments. Extending the arguments in the proofs of Theorems 4.4 and 4.5 in the obvious ways, it is easy to see that the increments must satisfy the following system of equations:

$$\begin{aligned} 2(2+\mu) - [(2+\mu)+y_1][1+e^{-y_1}] &= 0, \\ 2(4+\mu+\nu) - [(2+\mu)+y_1][1+e^{-y_1}] - [(2+\nu)+y_2][1+e^{-y_1-y_2}] &= 0, \\ 2c - [(2+\mu)y_1][1+e^{-y_1}] - [(2+\nu)+y_2][1+e^{-y_1-y_2}] & \\ -[(c-4-\mu-\nu)+y_3][1+e^{-y_1-y_2-y_3}] &= 0. \end{aligned} \tag{23}$$

International Electronic Journal of Pure and Applied Mathematics – IEJPAM, Volume 1, No. 3 (2010)

Evidently $y_1 = y_2 = y_3 = 0$ is a solution of (23) for all $\mu,\ \nu \geq 0$, and this corresponds to $\hat{x}$, which is a fixed point of F and therefore trivially a fixed point of F^2. It remains to find the nontrivial fixed points of F^2 near $\hat{x}$, which generate nontrivial 2-cycles of F for sufficiently small $\mu, \nu \geq 0$. We infer from Theorem 4.4 that along with $y_1 = 0$, there is pair of solutions $y_1^{(\pm)} = \phi^{(\pm)}(\sqrt{\mu}) = \pm\sqrt{6\mu} + O(\mu)$, where $\phi^{(\pm)}$ are analytic functions for sufficiently small $\mu \geq 0$. We now proceed to the second of equations (23) for each of $y_1 = 0,\ \phi^{(-)}(\sqrt{\mu})$ and $\phi^{(+)}(\sqrt{\mu})$. Substituting $y_1 = 0$ in the second equation of (23) yields

$$2(2+\nu) - [(2+\nu) + y_2][1 + e^{-y_2}] = 0. \tag{24}$$

Noting the similarity of (24) to the first equation of (23), it is clear that for $y_1 = 0$, the second equation of (23) has solutions $y_2 = 0$ and $y_2 = \phi^{(\pm)}(\sqrt{\nu})$ for all sufficiently small nonnegative ν. On the other hand, substituting $y_1 = \phi^{(\pm)}(\sqrt{\mu})$ in the second equation of (23) and using the fact that $\phi^{(\pm)}(\sqrt{\mu})$ are solutions of the first of equations (23), we readily compute that

$$2(2+\nu) - [(2+\nu) + y_2][1 + e^{-\phi^{(\pm)}(\sqrt{\mu}) - y_2}] = 0.$$

Then again applying our approach in the proof of Theorem 4.4, we find that for each of $\phi^{(-)}(\sqrt{\mu})$ and $\phi^{(+)}(\sqrt{\mu})$ there are three solutions; namely, $y_2 = \eta_{(+)}^{(-)}(\sqrt{\mu},\ \sqrt{\nu})$, $\eta_{(+)}^{(0)}(\sqrt{\mu},\ \sqrt{\nu}), \eta_{(+)}^{(+)}(\sqrt{\mu},\ \sqrt{\nu})$ for $y_1 = \phi^{(+)}(\sqrt{\mu})$ and $y_2 = \eta_{(-)}^{(-)}(\sqrt{\mu},\ \sqrt{\nu})$, $\eta_{(-)}^{(0)}(\sqrt{\mu},\ \sqrt{\nu}),\ \eta_{(-)}^{(+)}(\sqrt{\mu},\ \sqrt{\nu})$ for $y_1 = \phi^{(-)}(\sqrt{\mu})$. These solutions satisfy the following readily verified properties: all of the functions are analytic for sufficiently small $\mu,\ \nu \geq 0$,

$$\begin{aligned}\eta_{(-)}^{(-)}(\sqrt{\mu},\ \sqrt{\nu}) < \phi^{(-)}(\sqrt{\nu}) < \eta_{(+)}^{(-)}(\sqrt{\mu},\ \sqrt{\nu}) < \eta_{(-)}^{(0)}(\sqrt{\mu},\ \sqrt{\nu}) < 0 \\ < \eta_{(+)}^{(0)}(\sqrt{\mu},\ \sqrt{\nu}) < \eta_{(+)}^{(+)}(\sqrt{\mu},\ \sqrt{\nu}) < \phi^{(+)}(\sqrt{\nu}) < \eta_{(-)}^{(+)}(\sqrt{\mu},\ \sqrt{\nu}),\end{aligned} \tag{25}$$

for all sufficiently small $\mu,\ \nu > 0$, and $\eta_{(\pm)}^{(0,\ \pm)} = O(\sqrt{\mu},\ \sqrt{\nu})$ as $\mu,\ \nu \downarrow 0$. To summarize our analysis so far, we have found that the first two equations of (23) have the following nine solutions for sufficiently small nonnegative values of the parameters μ and ν: (i) $y_1 = y_2 = 0$; (ii) $y_1 = 0,\ y_2 = \phi^{(+)}(\sqrt{\nu})$; (iii) $y_1 = 0,\ y_2 = \phi^{(-)}(\sqrt{\nu})$; (iv) $y_1 = \phi^{(+)}(\sqrt{\mu}),\ y_2 = \eta_{(+)}^{(0)}(\sqrt{\mu},\ \sqrt{\nu})$; (v) $y_1 = \phi^{(+)}(\sqrt{\mu}),\ y_2 = \eta_{(+)}^{(+)}(\sqrt{\mu},\ \sqrt{\nu})$; (vi) $y_1 = \phi^{(+)}(\sqrt{\mu}),\ y_2 = \eta_{(+)}^{(-)}(\sqrt{\mu},\ \sqrt{\nu})$; (vii) $y_1 = \phi^{(-)}(\sqrt{\mu}),\ y_2 = \eta_{(-)}^{(0)}(\sqrt{\mu},\ \sqrt{\nu})$; (viii) $y_1 = \phi^{(-)}(\sqrt{\mu}),\ y_2 = \eta_{(-)}^{(+)}(\sqrt{\mu}, \sqrt{\nu})$; and (ix) $y_1 = \phi^{(-)}(\sqrt{\mu}),\ y_2 = \eta_{(-)}^{(-)}(\sqrt{\mu},\ \sqrt{\nu})$. It remains to solve the last equation of (23), where each of these nine solutions for the first two variables is substituted; this yields

$$\psi(y_3;\ \mu,\ \nu) := 2(c-b) - [(c-b) + y_3][1 + e^{-y_1(\sqrt{\mu},\ \sqrt{\nu}) - y_2(\sqrt{\mu},\ \sqrt{\nu}) - y_3}] = 0 \tag{26}$$

International Electronic Journal of Pure and Applied Mathematics – IEJPAM, Volume 1, No. 3 (2010)

where $y_1 = y_1(\sqrt{\mu},\ \sqrt{\nu})$, $y_2 = y_2(\sqrt{\mu},\ \sqrt{\nu})$ are known analytic functions of $(\sqrt{\mu},\ \sqrt{\nu})$ for sufficiently small $\mu,\ \nu \geq 0$ given in turn by each of the solutions (i)-(ix) of the first two equations. Now it follows from our assumption, $|1 - (c - b)| < 1$, that the same is true for all sufficiently small $\mu,\ \nu \geq 0$ in (26), which implies that

$$\frac{d\psi}{dy_3}(0;\ \mu,\ \nu) \neq 0,$$

and this completes the proof.